WSRC-TR-93-101

NRTSC
NUCLEAR REACTOR TECHNOLOGY
AND SCIENTIFIC COMPUTATIONS

KEYWORDS: LOPA LIMIT
LOPA CRITERION
FLOW EXCURSION
NATURAL CONVECTION
K-15.1 LIMITS
SPRIHTE TEST

RETENTION: PERMANENT

ANALYSIS OF SPRIHTE LOPA FLOW EXCURSION TESTS (U)

by

J. E. LAURINAT

ISSUED: FEBRUARY 1993

James E Laurinat 2-11-93
J. E. Laurinat, Authorized Derivative Classifier Date

SRL SAVANNAH RIVER LABORATORY, AIKEN, SC 29808
Westinghouse Savannah River Company
Prepared for the U. S. Department of Energy under
Contract DE-AC09-89SR18035

MASTER

DISTRIBUTION OF THIS DOCUMENT IS UNLIMITED

PROJECT:
DOCUMENT: WSRC-TR-93-101
TITLE: ANALYSIS OF SPRIHTE LOPA FLOW EXCURSION TESTS (U)
TASK: CONDUCT OF SHORT DURATION CRITICAL APPLICATION TECHNICAL WORK BY THE APPLIED REACTOR TECHNOLOGY GROUP
QA TASK NUMBER: 92-043-1
REVISION NUMBER: 0

APPROVALS

James E Laurinat — 2-11-93
J. E. LAURINAT, AUTHOR — DATE

K L Barbour — 2-11-93
K. L. BARBOUR, TECHNICAL REVIEWER — DATE

J D Menna — 2-22-93
J. D. MENNA, RESEARCH SUPERVISOR — DATE

A J Garrett — 3/1/93
A. J. GARRETT, RESEARCH MANAGER — DATE

TABLE OF CONTENTS

1.0 Summary 1

2.0 Description of SPRIHTE LOPA Tests 1

3.0 Description and Evaluation of the FLOPA Model for the SPRIHTE Tests 2

4.0 Selection of a Limit Criterion for the SPRIHTE Tests 3

5.0 Transition between High and Low Flow Rate Criterion 5

6.0 Conclusion 5

7.0 Acknowledgment 6

8.0 References 7

Appendix A Preparation of FLOPA Input for the Analysis of the SPRIHTE Tests A-1

A.1 Description of FLOPA Model of SPRIHTE Rig A-1

A.2 Differences Between Mark 22 and SPRIHTE Rig Models A-1

A.3 Application of the FLOPA Model of the SPRIHTE Rig A-5

A.4 Sample Input File for FLOPA Calculation of Flow Instability Limits for the SPRIHTE Tests A-7

A.5 Source Listing for SPRSPLIN A-14

A.6 Source Listing for SPRCOMB A-16

Appendix B Comparisons of Measured and Calculated Bulk Fluid Temperatures B-1

Appendix C Comparisons of Measured and Calculated Heater Wall Temperatures C-1

Appendix D Comparisons of Measured and Calculated Maximum Wall Temperatures D-1

LIST OF TABLES

Table 1 FLOPA Calculation of LOPA Limits for SPRIHTE Tests at 10 gpm and 25°C Inlet 8

Table 2 FLOPA Calculation of LOPA Limits for SPRIHTE Tests at 10 gpm and 40°C Inlet 9

Table 3 FLOPA Calculation of LOPA Limits for SPRIHTE Tests at 15 gpm and 25°C Inlet 10

Table 4 FLOPA Calculation of LOPA Limits for SPRIHTE Tests at 15 gpm and 0°C Inlet 11

Table 5 Comparisons between Measured Thermal Excursion Powers and Wall Saturation Temperature Criterion Limits Calculated Using the Concentric Flow Model 12

Table 6 Comparisons between Measured Thermal Excursion Powers and Wall Saturation Temperature Criterion Limits Calculated Using a Model with the Outer Channel Eccentricity Set to Match Calculated and Measured Differences between Hottest and Coldest Outer Channel Effluent Temperatures 13

Table 7 Margins between Measured Thermal Excursion Powers and Wall Saturation Temperature Criterion Limits Calculated Using the Concentric Flow Model 14

Table 8 Margins between Measured Thermal Excursion Powers and Wall Saturation Temperature Criterion Limits Calculated Using a Model with the Outer Channel Eccentricity Set to Match Calculated and Measured Differences between Hottest and Coldest Outer Channel Effluent Temperatures 15

Table 9 Wall Saturation Temperature Criterion Multipliers That Match Measured and Calculated Powers at Which the Maximum Wall Temperatures First Exceeded Saturation Temperatures, Based on Uncorrected Wall Temperature Measurements 16

Table 10 Wall Saturation Temperature Criterion Multipliers That Match Measured and Calculated Powers at Which the Maximum Wall Temperatures First Exceeded Saturation Temperatures, Based on Corrected Wall Temperature Measurements 17

Table 11 Variation of LOPA Limits with Wall Saturation Temperature Criterion Multiplier and Comparison with Current LOPA Stanton Number Limit 18

Table A-1 Comparison of Mark 22 Design and SPRIHTE Rig As-Built Dimensions .. A-1

Table A-2 Subchannel Dimensions for Eccentric Models of the Outer Channel of the SPRIHTE Rig A-5

Table A-3 Subchannel Pressure Loss Factors for Eccentric Models of the Outer Channel of the SPRIHTE Rig A-5

LIST OF FIGURES

Figure 1 Comparison of Wall Saturation Temperature Criterion Limits with Measured Conditions for the SPRIHTE Tests at 10 gpm and 25°C Inlet, Using Concentric Flow Channels. 19

Figure 2 Comparison of Wall Saturation Temperature Criterion Limits with Measured Conditions for the SPRIHTE Tests at 10 gpm and 40°C Inlet, Using Concentric Flow Channels. 20

Figure 3 Comparison of Wall Saturation Temperature Criterion Limits with Measured Conditions for the SPRIHTE Tests at 15 gpm and 25°C Inlet, Using Concentric Flow Channels. 21

Figure 4 Comparison of Wall Saturation Temperature Criterion Limits with Measured Conditions for the SPRIHTE Tests at 15 gpm and 40°C Inlet, Using Concentric Flow Channels. 22

Figure 5 Comparison of Wall Saturation Temperature Criterion Limits with Measured Conditions for the SPRIHTE Tests at 10 gpm and 25°C Inlet, Using Nominal Eccentricity for the Outer Flow Channel. 23

Figure 6 Comparison of Wall Saturation Temperature Criterion Limits with Measured Conditions for the SPRIHTE Tests at 10 gpm and 40°C Inlet, Using Nominal Eccentricity for the Outer Flow Channel. 24

Figure 7 Comparison of Wall Saturation Temperature Criterion Limits with Measured Conditions for the SPRIHTE Tests at 15 gpm and 25°C Inlet, Using Nominal Eccentricity for the Outer Flow Channel. 25

Figure 8 Comparison of Wall Saturation Temperature Criterion Limits with Measured Conditions for the SPRIHTE Tests at 15 gpm and 40°C Inlet, Using Nominal Eccentricity for the Outer Flow Channel. 26

Figure 9 Comparison of Wall Saturation Temperature Criterion Limits with Measured Conditions for the SPRIHTE Tests at 10 gpm and 25°C Inlet, Using Estimated Eccentricity for the Outer Flow Channel. 27

Figure 10 Comparison of Wall Saturation Temperature Criterion Limits with Measured Conditions for the SPRIHTE Tests at 10 gpm and 40°C Inlet, Using Estimated Eccentricity for the Outer Flow Channel. 28

Figure 11 Comparison of Wall Saturation Temperature Criterion Limits with Measured Conditions for the SPRIHTE Tests at 15 gpm and 25°C Inlet, Using Estimated Eccentricity for the Outer Flow Channel. 29

Figure 12 Comparison of Wall Saturation Temperature Criterion Limits with Measured Conditions for the SPRIHTE Tests at 15 gpm and 40°C Inlet, Using Estimated Eccentricity for the Outer Flow Channel. 30

Figure 13 Variation of Peclet Numbers in the Limiting Subchannel during the Inlet Header Break LOPA Transient for Subcycle K-15.1 31

LIST OF TABLES AND FIGURES (continued)

Figure A-1 Comparison of Measured Power Profile for the Outer Heater Tube with the Spline Fit Calculated by SPRSPLIN. A-17

Figure A-2 Comparison of Measured Power Profile for the Inner Heater Tube with the Spline Fit Calculated by SPRSPLIN. A-18

Figure A-3 Comparison of the Average Power Profile Calculated by SPRCOMB with Spline Fits for the Outer and Inner Heater Tubes. A-19

Figure B-1 Comparison of Measured and Calculated Subchannel Fluid Temperatures for the Inner Channel for the SPRIHTE Test at 10 gpm, 25°C Inlet, and 70 kW B-1

Figure B-2 Comparison of Measured and Calculated Subchannel Fluid Temperatures for the Middle Channel for the SPRIHTE Test at 10 gpm, 25°C Inlet, and 70 kW B-2

Figure B-3 Comparison of Measured and Calculated Subchannel Fluid Temperatures for the Outer Channel for the SPRIHTE Test at 10 gpm, 25°C Inlet, and 70 kW B-3

Figure B-4 Comparison of Measured and Calculated Subchannel Fluid Temperatures for the Inner Channel for the SPRIHTE Test at 10 gpm, 40°C Inlet, and 51 kW B-4

Figure B-5 Comparison of Measured and Calculated Subchannel Fluid Temperatures for the Middle Channel for the SPRIHTE Test at 10 gpm, 40°C Inlet, and 51 kW B-5

Figure B-6 Comparison of Measured and Calculated Subchannel Fluid Temperatures for the Outer Channel for the SPRIHTE Test at 10 gpm, 40°C Inlet, and 51 kW B-6

Figure B-7 Comparison of Measured and Calculated Subchannel Fluid Temperatures for the Inner Channel for the SPRIHTE Test at 15 gpm, 25°C Inlet, and 141 kW B-7

Figure B-8 Comparison of Measured and Calculated Subchannel Fluid Temperatures for the Middle Channel for the SPRIHTE Test at 15 gpm, 25°C Inlet, and 141 kW B-8

Figure B-9 Comparison of Measured and Calculated Subchannel Fluid Temperatures for the Outer Channel for the SPRIHTE Test at 15 gpm, 25°C Inlet, and 141 kW B-9

Figure B-10 Comparison of Measured and Calculated Subchannel Fluid Temperatures for the Inner Channel for the SPRIHTE Test at 15 gpm, 40°C Inlet, and 78 kW B-10

LIST OF TABLES AND FIGURES (continued)

Figure B-11 Comparison of Measured and Calculated Subchannel Fluid Temperatures for the Middle Channel for the SPRIHTE Test at 15 gpm, 40°C Inlet, and 78 kW..... B-11

Figure B-12 Comparison of Measured and Calculated Subchannel Fluid Temperatures for the Outer Channel for the SPRIHTE Test at 15 gpm, 40°C Inlet, and 78 kW..... B-12

Figure C-1 Comparison of Measured and Calculated Inner Heater Wall Temperatures for the SPRIHTE Test at 15 gpm, 40°C Inlet, and 78 kW..... C-1

Figure C-2 Comparison of Measured and Calculated Outer Heater Wall Temperatures for the SPRIHTE Test at 15 gpm, 40°C Inlet, and 78 kW..... C-2

Figure C-3 Comparison of Measured and Calculated Inner Heater Wall Temperatures for the SPRIHTE Test at 15 gpm, 40°C Inlet, and 142 kW..... C-3

Figure C-4 Comparison of Measured and Calculated Outer Heater Wall Temperatures for the SPRIHTE Test at 15 gpm, 40°C Inlet, and 142 kW..... C-4

Figure D-1 Comparison of Measured and Calculated Maximum Wall Temperatures for the SPRIHTE Tests at 10 gpm and 25°C Inlet..... D-1

Figure D-2 Comparison of Measured and Calculated Maximum Wall Temperatures for the SPRIHTE Tests at 10 gpm and 40°C Inlet..... D-2

Figure D-3 Comparison of Measured and Calculated Maximum Wall Temperatures for the SPRIHTE Tests at 15 gpm and 25°C Inlet..... D-3

Figure D-4 Comparison of Measured and Calculated Maximum Wall Temperatures for the SPRIHTE Tests at 15 gpm and 40°C Inlet..... D-4

1.0 Summary

The SPRIHTE FLOPA flow excursion tests have been modeled using FLOPA, the assembly thermal-hydraulics limits analysis code for the LOPA. FLOPA calculations show $T_{wall} = T_{sat}$ is a reliable precursor to the onset of thermal excursion at prototypic flow rates during the ECS addition phase of the LOPA [1].

A FLOPA model was created based on nominal dimensions for the SPRIHTE rig and an assumption that the rig's cylinders were concentrically located. This model can determine when $T_{wall} = T_{sat}$ if adjustments are made to account for differences between measured and calculated subchannel flow and heat transfer rates. To make these adjustments, a multiplier β was applied to the wall saturation temperature criterion ($T_{wall} = \beta\ T_{sat}$, in degrees C) to match measured and calculated powers at which the saturation temperature was first exceeded at the wall. Based on preliminary test results, a multiplier of 0.878 was recommended for use in calculating LOPA limits for the K-15.1 subcycle. This multiplier provides margins of 14% to 19% between the calculated wall saturation temperature limits and the measured powers at the onset of thermal excursion. The effective margins used in the final LOPA limits, which include dimensional and heat transfer model uncertainties and biases due to eccentricities, range from 38% to 41%.

It is estimated that use of the wall saturation temperature criterion lowers the K-14.1 subcycle LOPA core power limit, which is based on a Stanton number of 0.0025, from 41% to 37% of the historical full power of 2400 MW.

2.0 Description of SPRIHTE LOPA Tests

The SPRIHTE test rig originally was used for LOCA-ECS tests. Later, the rig was used to conduct a series of LOPA flow excursion tests [2,3]. The LOPA tests were single-phase liquid flow excursion tests, while in the LOCA-ECS tests entrained air was introduced into the test section. The SPRIHTE FLOPA tests were added to obtain a prototypical database for the limit criterion during the low flow, ECS addition phase of the LOPA. The criterion for the K-14.1 subcycle, St = 0.0025, was based on flow excursion tests conducted in Rig FC [4], which consisted of a single ribbed annulus heated from the outside wall.

The SPRIHTE test rig was constructed to be prototypic of a Mark 22 assembly. The SPRIHTE rig differed from a Mark 22, however, in that the there was no USH. The purge channel between the outer target tube and the USH was replaced by two external bypass tubes located on opposite sides of the heated section. In addition, only the middle two tubes of the SPRIHTE rig, corresponding to the inner and outer fuel tubes of a Mark 22, were heated. The outer tube received 60% of the electrical power, and the inner tube received 40%.

During the SPRIHTE tests the flow rate and the inlet temperature were held constant and the power was increased in increments until a thermal excursion was detected by wall thermocouples. Downward flow through the test section was maintained by a centrifugal pump with a high impedance. Prior to thermal excursion, fluid thermocouple measurements indicated that there was flow reversal (upflow) in the outer flow channel. The thermal excursion always occurred in this outer channel.

Tests were conducted at flow rates of 5, 10, and 15 gpm and at inlet temperatures of 25°C and 40°C. Only the 10 and 15 gpm tests have been analyzed, since these flow rates are

within the flow range at which the limit for the ECS addition phase of the LOPA is set [1].

3.0 Description and Evaluation of the FLOPA Model for the SPRIHTE Tests

The FLOPA model for the SPRIHTE rig used the same geometry and pressure loss coefficients as were used in the LOPA limits calculations. Differences between nominal Mark 22 and as-built tube diameters were small and were therefore ignored. It was assumed that the surface roughness of the SPRIHTE test rig tubes was the same as that of a Mark 22 and that the heated section inlet and bottom end fittings were prototypic. The use of prototypic Mark 22 dimensions and nominal friction and form loss factors was justified through comparisons of measured and calculated fluid and wall temperatures under stable flow conditions. These comparisons showed that the use of nominal dimensions and loss factors did not have a significant adverse effect on the ability of the FLOPA code to predict these temperatures.

The effects of thermocouple insertions on the flow in the inner and outer channels was assumed to be negligible, and corrections to fluid thermocouple measurements to account for fluid temperature gradients were not considered. Corrections to wall thermocouple measurements to account for thermal gradients in the heater tubes also were ignored. The wall thermocouples were centered within the heated walls. Subsequent calculations using the new limit criterion for the SPRIHTE tests showed that the difference between the center wall and surface temperatures was 0.3°C at limit conditions. This difference was judged to be insignificant.

Finally, in calculations to determine a limit criterion, the SPRIHTE test rig was modeled as a series of concentric annuli. Differences among subchannel fluid temperature measurements, particularly for the outer channel, indicated that the SPRIHTE rig cylinders may have been eccentrically located. However, no credit was taken for this apparent eccentricity in the limit criterion analysis, since the degree of eccentricity was not measured under heated conditions.

To determine the effect of eccentricity, three-dimensional, eccentric FLOPA models were used. Three models were created. In the first, the eccentricity of the outer channel was set to match the calculated difference between the hottest and coldest subchannel in the outer channel with the measured difference. In the second, the eccentricity of the outer channel was set at its maximum value allowed by the rib tip clearance. Finally, a model was created in which the eccentricities in all three flow channels were set at the maximum values allowed by rib tip clearances. The eccentric channels were aligned in the same radial direction to maximize differences in subchannel heat transfer rates. This last model is used in LOPA limits calculations.

Appendix A presents details of the calculations used to create the FLOPA input files and contains a sample input file.

To verify that the FLOPA calculations accurately modeled flow and heat transfer in the SPRIHTE rig, calculated and measured values for subchannel fluid and heated wall temperatures were compared. In these comparisons, the eccentricity of the outer channel was adjusted to match calculated and measured differences between the hottest and coldest subchannel effluent temperatures. A separate match was performed for a heated stable flow test at each test condition. Figures B-1 through B-12 in Appendix B compare fluid temperature profiles for the inner, middle, and outer channels under stable flow conditions. The results in these figures show that FLOPA models flow and heat transfer to the coolant within a range of about 5°C. Figures C-1 and C-2 in Appendix C compare

inner and outer heater wall temperature profiles for the stable flow test condition at 15 gpm and 40°C inlet. Again, the FLOPA model predicts measured temperatures within about 5°C. Figures C-3 and C-4 compare these wall temperatures at a higher power, where flow became unstable in the outer channel. (Unstable flow was detected by means of fluctuations of about 5°C in the effluent temperature.) In these cases, measured wall temperatures for two of the outer subchannels are higher than the calculated temperatures, and the measured wall temperatures for the inner channel are lower than the calculated temperatures.

4.0 Selection of a Limit Criterion for the SPRIHTE Tests

The current limit criterion for the ECS addition phase of the LOPA (St = 0.0025) was selected to bound the onset of unstable flow for a previous series of LOPA low flow flow excursion tests conducted in Rig FC [4]. However, this criterion does not provide a lower bound to the onset of unstable flow in the outer channel of the SPRIHTE test rig. At powers lower than those given by the Stanton number criterion, the outer channel fluid temperature measurements fluctuated with time and, in at least one subchannel, showed evidence of flow reversal.

Based on the results of the SPRIHTE tests, it was decided to change both the criterion and the bounding phenomenon for the ECS addition phase of the LOPA. The Stanton number criterion was changed to a criterion that the wall temperature not exceed the fluid saturation temperature. This wall saturation temperature criterion ensures that there is no boiling along the heated walls and, therefore, a thermal excursion cannot occur. Accordingly, the bounding phenomenon was changed from the onset of unstable flow to the onset of thermal excursion. The new criterion permits unstable flow provided that conditions for the onset of a thermal excursion are not exceeded.

In evaluating the wall saturation temperature criterion, a multiplier was added to account for differences between measured and calculated subchannel flow and heat transfer rates up to the point where unstable flow and possible flow reversal occur (see the discussion of wall temperature distributions in the preceding section). The limiting fluid temperature, in degrees C, is the product of this multiplier and the saturation temperature in degrees C.

Measured and computed maximum wall temperatures were compared to verify that FLOPA could accurately calculate the wall saturation temperature criterion. The maximum temperatures for these comparisons were located on the outer wall of the outer heater (the inner wall of the outer flow channel). Figures D-1 through D-4 in Appendix D illustrate these comparisons for four cases: 1) concentric flow channels, 2) an estimated eccentricity in the outer channel set to match calculated and measured differences between the hottest and coldest subchannel effluent temperatures, 3) the maximum degree of eccentricity in the outer channel allowed by the rib tip clearance, and 4) the maximum degree of eccentricity allowed by the rib tip clearance in all channels. The final case, in which the eccentricity in each flow channel is aligned so that the subchannels with the smallest cross-sectional areas are located on the same side of the assembly, is used to perform LOPA limits calculations. For the estimated eccentricity case (Case 2), the FLOPA model accurately predicts the maximum wall temperature at low powers under steady flow conditions, but underestimates the maximum temperatures by as much as 10°C at higher powers.

Tables 1 through 4 compare measured flow conditions with limiting conditions based on the Stanton number and wall saturation temperature criteria. All measured conditions are listed. Powers where unstable flow and flow reversal were first detected in the outer

channel are noted, as are the powers where the maximum measured wall temperature first exceeded the fluid saturation temperature and where thermal excursions took place. The onsets of unstable flow, flow reversal, and thermal excursion occurred somewhere between these power levels and the next lower powers. The powers at which the maximum wall temperature equaled the saturation temperature were determined by linear interpolation of measurements at different test conditions.

Also listed in Tables 1 and 2 are conditions where FLOPA computed flow reversal in one subchannel of the outer channel (Channel 4). Limits were computed for three cases, one with concentric flow channels, one with a maximum allowable degree of eccentricity in the outer flow channel to account for the nominal rib tip clearance between the outer heater tube and the outer housing of the test section, and one with an eccentricity that matched calculated and measured temperature differences between the hottest and coldest subchannel temperatures in the outer channel. For the eccentric cases at 10 gpm, the FLOPA code predicted that flow reversal would occur in one subchannel of the outer channel (Channel 4). FLOPA did not predict that flow reversal would occur prior to measured thermal excursion conditions at 15 gpm.

Figures 1 through 12 illustrate the comparisons between measured conditions and calculated limits listed in Tables 1 through 4. These figures compare limits for the wall saturation temperature criterion with different multipliers with measured stable flow, unstable flow, flow reversal, and thermal excursion conditions and the calculated Stanton number limit. Figures 1 through 4 make these comparisons for a concentric channel model, Figures 5 through 8 make comparisons for the maximum outer channel eccentricity based on rib tip clearances, and Figures 9 through 12 make comparisons for an outer channel eccentricity that matches calculated and measured temperature differences between the hottest and coldest subchannel effluent temperatures.

Tables 5 and 6 summarize comparisons between wall saturation temperature limits for different multipliers and powers at which the onsets to unstable flow, flow reversal, and thermal excursions occurred. Table 5 compares measured powers with limits calculated using the concentric FLOPA model. Table 6 compares powers for limits calculated using a model in which the outer channel eccentricity was set to match measured and calculated spreads in subchannel effluent temperatures. Both nominal limiting powers and limiting powers with uncertainties are tabulated for the concentric model. The nominal limits were calculated using FLOPA with the wall saturation temperature criterion. The limits with uncertainty were computed by multiplying the nominal limits by the ratio of the LOPA limit with uncertainties and biases to the best estimate LOPA limit for K-15.1. Uncertainties for heated length, friction factor, fuel tube power fraction, the turbulent heat transfer coefficient, and tube thicknesses, and a bias due to eccentricity were included. Limits are listed for multipliers ranging from 0.8 to 1.0. Tables 7 and 8 list margins between the wall saturation temperature limits and the measured powers at the onset of thermal excursion. For the K-15.1 limit multiplier (see the following discussion), the margin for the nominal limit ranges between 14% and 19% for the concentric model and 19% and 24% for the eccentric model. The margin for the limit with uncertainties ranges between 38% and 41% for the concentric model.

Linear interpolations were performed to determine multipliers to match measured and calculated powers at which the maximum wall temperature first exceeded the saturation temperature. The powers for these interpolations were calculated based on both concentric flow channel dimensions and an outer channel eccentricity set to match the spread in computed and measured subchannel effluent temperatures under stable flow conditions.

Two interpolations were performed. The first interpolation used preliminary data [2]. It was performed to obtain a multiplier in time to calculate the LOPA limit for Subcycle K-15.1. The second interpolation used final, certified data [3] and was performed to verify the results of the first interpolation. Table 9 lists the results of the first interpolation, and Table 10 lists the results of the second interpolation. The preliminary and final values for the multiplier differ due to the presence of a bias in the preliminary wall temperature measurements [3] and the fact that more test conditions are included in the final results than in the preliminary results. Removal of the wall temperature bias lowered the wall temperature measurements, so that the powers at which the final wall temperatures reached saturation were higher than the powers at which the preliminary temperatures reached saturation. This made the final values of the wall saturation temperature criterion multiplier greater than the preliminary values. The addition of more test conditions also changed the interpolated value of the multiplier. The change was most significant for tests at 10 gpm and 40°C inlet, for which the final value of the multiplier was significantly less than the preliminary value.

The multiplier for the wall saturation temperature criterion was based on the calculated results for concentric channels. Based on the preliminary results a wall saturation temperature criterion multiplier of 0.878 was recommended for calculating K-15.1 LOPA ECS addition phase limits. For the four tests analyzed in this report, this is the average value of the multiplier that matches measured and calculated powers at which the maximum wall temperature equals the saturation temperature. As indicated in Table 7 , the margins between the limiting power for this value of the multiplier and the power at thermal excursion are between 14% and 19%. As shown in Table 8, FLOPA predicts powers 19% to 24% below those at thermal excursion using the nominal eccentric flow model with this value of the multiplier.

Table 11 gives the effect of the wall saturation temperature multiplier on the limit for the ECS addition phase of the LOPA. According to the results in this table, a multiplier of 0.878 would yield a limiting power that is 37% of historical full power, based on K-14.1 limits calculations. This power is less than the K-14.1 LOPA limit of 41% of historical full power [1]. Table 11 also lists assembly flow rates at the nominal limiting conditions. These flow rates are within the range of test section flow rates for the SPRIHTE tests.

5.0 Transition between High and Low Flow Rate Criterion

The wall saturation temperature criterion is applicable only at low flow rates, where the SPRIHTE tests have demonstrated that buoyancy-induced flow reversal can occur prior to the onset of flow instability. A Stanton number criterion should be retained for use at higher flow rates, where buoyancy effects are not significant. It is suggested that the use of the wall saturation temperature criterion be restricted to Peclet numbers below 70,000. This value corresponds to the lowest Peclet number tested in benchmarking the LOCA-FI Stanton number criterion (St = 0.00455) [5] and is considerably above the value where buoyancy effects are significant.

The current structure of the FLOPA limits code makes it easier to specify when to apply the wall saturation temperature criterion in terms of a transient time instead of a Peclet number. Figure 13 depicts variations in the Peclet numbers in the limiting subchannel (located outside the outer fuel tube of the Mark 22 assembly) for the inlet header break LOPA transient. According to the results in this figure, the wall saturation temperature criterion can be applied 344 seconds after the start of the LOPA transient, when the DC pump motors flood and the DC pumps begin to coast down. The Peclet number at this time is approximately 70,000.

6.0 Conclusion

Based on the results of the SPRIHTE tests, it is recommended that a wall saturation temperature criterion should be used for the limit for the ECS addition phase of the LOPA. An analysis of preliminary test results was used to set this criterion for the K-15.1 subcycle limit. This analysis shows that the maximum wall temperature inside the assembly should not exceed 0.878 times the local fluid saturation temperature in degrees C. This multiplier provides margins of 14% to 19% between the calculated wall saturation temperature limits and the measured powers at the onset of thermal excursion. The effective margins used in the final LOPA limits, which include dimensional and heat transfer model uncertainties and biases due to eccentricities, range from 38% to 41%.

The use of this wall saturation temperature criterion would lower the low flow LOPA limit for the K-14.1 subcycle, which is based on a Stanton number criterion (St = 0.0025), from 41% to 37% of historic full power.

Additional analyses may be needed to develop better understanding of the mechanisms leading to thermal excursions at the SPRIHTE test conditions.

7.0 Acknowledgment

The assistance of P. K. Paul in performing the FLOPA calculations to model the SPRIHTE test rig and in providing suggestions for analyzing the results of those calculations is appreciated.

8.0 References

1. P. K. Paul and K. L. Barbour, "DEGB LOPA Limit Recommendation for the K-14.1 Subcycle," WSRC-RP-91-444, Rev. 1, July, 1992.

2. H. N. Guerrero, "Transmittal of Preliminary SPRIHTE LOPA Test Data," NES-ETH-920346, October 8, 1991.

3. H. N. Guerrero and C. M. Hart, "SPRIHTE Prototypic Assembly LOPA Test Data Report," WSRC-TR-93-012, January, 1993.

4. B. S. Johnston, "Limits for Stable Downward Flow in a Single Heated Annulus at LOPA Conditions," NES-ETH-910190, March 25, 1991.

5. J. A. Block, C. J. Crowley, F. X. Dolan, R. G. Sam, and B. H. Stoedefalke, "Nucleate Boiling Pressure Drop in an Annulus," Creare, Inc., Technical Note TN-499, Vol. 1, October, 1990.

6. P. K. Paul, Laboratory Notebook WSRC-NB-92-107, page 80.

7. K. L. Barbour, "Inlet Header Break: Revised 30% Mass Flow Reduction Bias, Rev. 1," NES-ART-920070, March 6, 1992.

8. W. M. Massey, NES-ART-900122, August 16, 1990.

9. H. N. Guerrero, "Prototypic Assembly Mockup Receipt Inspection and Verification," NRTSC Technical Procedure No. TP-90-003, Rev. 1, August 3, 1990.

10. H. N. Guerrero, "SPRIHTE 2 Heat Flux Profile," NES-ETH-930011, January 14, 1991.

11. L. D. Koffman, "Analysis of CMX Hydraulic Data for the Mark 22 (U)," DPST-88-975, December, 1988.

12. C. M. Hart, "SPRIHTE 2 Dimensional References," NES-ETH-930006, January 14, 1993.

13. A. M. White, "Analysis of the Effect of Eccentricity on the Uncertainty in Reactor Power Limits," DPST-88-738, July, 1988.

Table 1. FLOPA Calculation of LOPA Limits for SPRIHTE Tests at 10 gpm and 25°C Inlet

Measured Conditions

Power	Measured Condition
69.8	Stable Flow
106.8	Unstable Flow, Flow Reversal in Outer Channel
129.8	----------
130.8	Maximum Wall Temperature = Saturation Temperature*
140.1	----------
152.4	----------
160.6	Thermal Excursion in Outer Channel**

FLOPA Calculated Results

Condition	Power (kW)	Nom. Lim. St in Ch. 4	ONB Ratio
Concentric Flow Channels			
Stanton Number Limit	150.7	0.00250	0.570
Wall Sat'n. Temp. Limit	157.4	0.00279	0.607
0.9*Wall Sat'n. Temp. Limit	135.2	0.00193	0.494
0.85*Wall Sat'n. Temp. Limit	123.9	0.00163	0.445
0.8*Wall Sat'n. Temp. Limit	112.7	0.00138	0.399
Nominal Eccentricity in Outer Channel* **			
Stanton Number Limit	117.8	0.00250	0.541
Flow Reversal	118.0	0.00254	0.545
Wall Sat'n. Temp. Limit****	132.3	0.00287	0.634
0.9*Wall Sat'n. Temp. Limit	115.6	0.00221	0.511
0.85*Wall Sat'n. Temp. Limit	109.2	0.00179	0.456
0.8*Wall Sat'n. Temp. Limit	101.3	0.00147	0.407
Estimated Eccentricity in Outer Channel***			
Stanton Number Limit	134.0	0.00250	0.558
Flow Reversal	137.0	0.00286	0.601
Wall Sat'n. Temp. Limit****	134.8	0.00282	0.633
0.9*Wall Sat'n. Temp. Limit	126.6	0.00203	0.499
0.85*Wall Sat'n. Temp. Limit	117.6	0.00169	0.446
0.8*Wall Sat'n. Temp. Limit	107.9	0.00141	0.399

*This power was estimated by linear interpolation of maximum measured wall temperatures at different test conditions.
**Actual flow was 8.7 gpm for this case.
***The nominal eccentricity is the amount of eccentricity that is present if two adjacent ribs of the outer housing contact the outer tube, based on nominal rib tip clearances for the Mark 22 assembly.
****In the calculation of this limit flow reversal was predicted to occur in one subchannel in the outer flow channel. The FLOPA code does not model flow and heat transfer accurately for reverse flows.
*****The estimated eccentricity was set to match the calculated difference between the hottest and coldest subchannel effluent temperature in the outer channel with the measured difference. This eccentricity is about half the nominal eccentricity. Appendix A details the calculation of this eccentricity and Table A-2 lists the results of those calculations.

Table 2. FLOPA Calculation of LOPA Limits for SPRIHTE Tests at 10 gpm and 40°C Inlet

Measured Conditions

Power	Measured Condition
51.3	Stable Flow
61.9	Stable Flow
74.1	Unstable Flow in Outer Channel
80.7	Flow Reversal in Outer Channel
87.7	---
92.4	Maximum Wall Temperature = Saturation Temperature*
93.8	---
100.8	---
114.1	---
121.9	---
127.1	Thermal Excursion in Outer Channel
131.5	---

FLOPA Calculated Results

Condition	Power (kW)	Nom. Lim. St in Ch. 4	ONB Ratio
Concentric Flow Channels			
Stanton Number Limit	123.1	0.00250	0.522
Wall Sat'n. Temp. Limit	128.7	0.00279	0.558
0.9*Wall Sat'n. Temp. Limit	107.2	0.00182	0.434
0.85*Wall Sat'n. Temp. Limit	96.4	0.00149	0.381
0.8*Wall Sat'n. Temp. Limit	85.5	0.00123	0.332
Nominal Eccentricity in Outer Channel**			
Stanton Number Limit	98.0	0.00250	0.496
Flow Reversal	99.0	0.00268	0.514
Wall Sat'n. Temp. Limit***	104.6	0.00294	0.586
0.9*Wall Sat'n. Temp. Limit	94.5	0.00199	0.441
0.85*Wall Sat'n. Temp. Limit	86.7	0.00158	0.382
0.8*Wall Sat'n. Temp. Limit	78.0	0.00127	0.330
Estimated Eccentricity in Outer Channel****			
Stanton Number Limit	110.3	0.00250	0.506
Flow Reversal	117.0	0.00318	0.591
Wall Sat'n. Temp. Limit	115.4	0.00298	0.565
0.9*Wall Sat'n. Temp. Limit	100.4	0.00190	0.431
0.85*Wall Sat'n. Temp. Limit	91.3	0.00154	0.376
0.8*Wall Sat'n. Temp. Limit	81.6	0.00125	0.325

*This power was estimated by linear interpolation of maximum measured wall temperatures at different test conditions.
**The nominal eccentricity is the amount of eccentricity that is present if two adjacent ribs of the outer housing contact the outer tube, based on nominal rib tip clearances for the Mark 22 assembly.
***In the calculation of this limit flow reversal was predicted to occur in one subchannel in the outer flow channel. The FLOPA code does not model flow and heat transfer accurately for reverse flows.
****The estimated eccentricity was set to match the calculated difference between the hottest and coldest subchannel effluent temperature in the outer channel with the measured difference. This eccentricity is about half the nominal eccentricity. Appendix A details the calculation of this eccentricity and Table A-2 lists the results of those calculations.

Table 3. FLOPA Calculation of LOPA Limits for SPRIHTE Tests at 15 gpm and 25°C Inlet

Measured Conditions

Power	Measured Condition
141.3	Stable Flow
175.9	Stable Flow
183.2	Unstable Flow in Outer Channel
187.6	----------
193.7	----------
197.3	Flow Reversal in Outer Channel
199.1	Maximum Wall Temperature = Saturation Temperature*
208.3	----------
213.8	----------
224.0	----------
226.8	----------
231.4	Thermal Excursion in Outer Channel

FLOPA Calculated Results

Condition	Power (kW)	Nom. Lim. St in Ch. 4	ONB Ratio
Concentric Flow Channels			
Stanton Number Limit	232.2	0.00250	0.627
Wall Sat'n. Temp. Limit	232.2	0.00250	0.627
0.9*Wall Sat'n. Temp. Limit	197.5	0.00176	0.511
0.85*Wall Sat'n. Temp. Limit	180.5	0.00150	0.461
0.8*Wall Sat'n. Temp. Limit	163.7	0.00127	0.414
Nominal Eccentricity in Outer Channel**			
Stanton Number Limit	201.7	0.00250	0.593
Flow Reversal	----		
Wall Sat'n. Temp. Limit	208.6	0.00276	0.626
0.9*Wall Sat'n. Temp. Limit	180.7	0.00188	0.506
0.85*Wall Sat'n. Temp. Limit	166.3	0.00157	0.456
0.8*Wall Sat'n. Temp. Limit	151.5	0.00132	0.408
Estimated Eccentricity in Outer Channel***			
Stanton Number Limit	215.3	0.00250	0.603
Flow Reversal	----		
Wall Sat'n. Temp. Limit	219.5	0.00263	0.621
0.9*Wall Sat'n. Temp. Limit	188.6	0.00182	0.503
0.85*Wall Sat'n. Temp. Limit	172.9	0.00154	0.452
0.8*Wall Sat'n. Temp. Limit	157.3	0.00130	0.405

*This power was estimated by linear interpolation of maximum measured wall temperatures at different test conditions.
**The nominal eccentricity is the amount of eccentricity that is present if two adjacent ribs of the outer housing contact the outer tube, based on nominal rib tip clearances for the Mark 22 assembly.
***The estimated eccentricity was set to match the calculated difference between the hottest and coldest subchannel effluent temperature in the outer channel with the measured difference. This eccentricity is about half the nominal eccentricity. Appendix A details the calculation of this eccentricity and Table A-2 lists the results of those calculations.

Table 4. FLOPA Calculation of LOPA Limits for SPRIHTE Tests at 15 gpm and 40°C Inlet

Measured Conditions

Power	Measured Condition
77.8	Stable Flow
91.4	Stable Flow
132.2	Unstable Flow in Outer Channel
142.4	----------
151.8	Flow Reversal in Outer Channel
161.0	----------
164.1	Maximum Wall Temperature = Saturation Temperature*
171.5	----------
181.8	----------
188.2	Thermal Excursion in Outer Channel

FLOPA Calculated Results

Condition	Power (KW)	Nom. Lim. St in Ch. 4	ONB Ratio
Concentric Flow Channels			
Stanton Number Limit	191.3	0.00250	0.567
Wall Sat'n. Temp. Limit	193.2	0.00256	0.575
0.9*Wall Sat'n. Temp. Limit	159.1	0.00170	0.449
0.85*Wall Sat'n. Temp. Limit	142.4	0.00140	0.394
0.8*Wall Sat'n. Temp. Limit	125.9	0.00115	0.344
Nominal Eccentricity in Outer Channel**			
Stanton Number Limit	175.2	0.00250	0.542
Flow Reversal	----		
Wall Sat'n. Temp. Limit	180.9	0.00272	0.568
0.9*Wall Sat'n. Temp. Limit	150.5	0.00175	0.441
0.85*Wall Sat'n. Temp. Limit	135.1	0.00142	0.386
0.8*Wall Sat'n. Temp. Limit	119.8	0.00116	0.336
Estimated Eccentricity in Outer Channel***			
Stanton Number Limit	173.2	0.00250	0.541
Flow Reversal	----		
Wall Sat'n. Temp. Limit	179.1	0.00274	0.569
0.9*Wall Sat'n. Temp. Limit	149.1	0.00175	0.441
0.85*Wall Sat'n. Temp. Limit	134.0	0.00142	0.386
0.8*Wall Sat'n. Temp. Limit	118.8	0.00116	0.336

*This power was estimated by linear interpolation of maximum measured wall temperatures at different test conditions.

**The nominal eccentricity is the amount of eccentricity that is present if two adjacent ribs of the outer housing contact the outer tube, based on nominal rib tip clearances for the Mark 22 assembly.

***The estimated eccentricity was set to match the calculated difference between the hottest and coldest subchannel effluent temperature in the outer channel with the measured difference. This eccentricity is slightly greater than the nominal eccentricity. Appendix A details the calculation of this eccentricity and Table A-2 lists the results of those calculations.

Table 5. Comparisons between Measured Thermal Excursion Powers and Wall Saturation Temperature Criterion Limits Calculated Using the Concentric Flow Model

Flow Rate (gpm)	Inlet Temp. (°C)	Power at Onset of Unstable Flow (kW)*	Power at Onset of Flow Reversal (kW)*	Power at Onset of Thermal Excursion (kW)*	Wall Sat'n. Temp. Criterion Multiplier	Nominal Calculated Limit (kW)**	Calculated Limit with Uncertainties (kW)***
10	25	69.8 to 106.8	69.8 to 106.8	152.4 to 160.6	1.00	157.4	115.0
					0.90	135.2	98.7
					0.878	130.2	95.1
					0.85	123.9	90.5
					0.80	112.7	82.3
10	40	61.9 to 74.1	74.1 to 80.7	121.9 to 127.1	1.00	128.7	94.0
					0.90	107.2	78.3
					0.878	102.4	74.8
					0.85	96.4	70.4
					0.80	85.5	62.4
15	25	175.9 to 183.2	193.7 to 197.3	226.8 to 231.4	1.00	232.2	169.6
					0.90	197.5	144.2
					0.878	190.0	138.8
					0.85	180.5	131.8
					0.80	163.7	119.6
15	40	91.4 to 132.2	142.4 to 151.8	181.8 to 188.2	1.00	193.2	141.1
					0.90	159.1	116.2
					0.878	151.8	110.8
					0.85	142.4	104.0
					0.80	125.9	91.9

*The lower power listed is the highest measured power before the onset of unstable flow, flow reversal, or thermal excursion. The higher power listed is the lowest measured power after the onset of these conditions.

**The nominal limit is the wall saturation temperature limit calculated by FLOPA.

***The calculated limit with uncertainties is the estimated final limit after the application of uncertainties and biases in the LOPA limits analysis. This limit includes the effects of uncertainties in the heated length, the friction factor, the tube power fractions, the turbulent heat transfer coefficient, and tube thicknesses [6] and a bias due to eccentrically located tubes. The bias due to eccentricity was computed by comparing nominal limits for the ECS addition phase of the K-15.1 subcycle for concentrically and eccentrically located tubes. In the eccentric limit calculation, the maximum degree of eccentricity allowed by nominal rib tip clearances was used for all cylinders.

Table 6. Comparisons between Measured Thermal Excursion Powers and Wall Saturation Temperature Criterion Limits Calculated Using a Model with the Outer Channel Eccentricity Set to Match Calculated and Measured Differences between Hottest and Coldest Outer Channel Effluent Temperatures

Flow Rate (gpm)	Inlet Temp. (°C)	Power at Onset of Unstable Flow (kW)*	Power at Onset of Flow Reversal (kW)*	Power at Onset of Thermal Excursion (kW)*	Wall Sat'n. Temp. Criterion Multiplier	Nominal Calculated Limit (kW)**
10	25	69.8 to 106.8	69.8 to 106.8	152.4 to 160.6	1.00	134.8
					0.90	126.6
					0.878	122.6
					0.85	117.6
					0.80	107.9
10	40	61.9 to 74.1	74.1 to 80.7	121.9 to 127.1	1.00	115.4
					0.90	100.4
					0.878	96.4
					0.85	91.3
					0.80	81.6
15	25	175.9 to 183.2	193.7 to 197.3	226.8 to 231.4	1.00	219.5
					0.90	188.6
					0.878	181.7
					0.85	172.9
					0.80	157.3
15	40	91.4 to 132.2	142.4 to 151.8	181.8 to 188.2	1.00	179.1
					0.90	149.1
					0.878	142.5
					0.85	134.0
					0.80	118.8

*The lower power listed is the highest measured power before the onset of unstable flow, flow reversal, or thermal excursion. The higher power listed is the lowest measured power after the onset of these conditions.

**The nominal limit is the wall saturation temperature limit calculated by FLOPA, using a model in which the outer channel eccentricity is set to match measured and calculated differences between the hottest and coldest subchannel effluent temperatures.

Table 7. Margins between Measured Thermal Excursion Powers and Wall Saturation Temperature Criterion Limits Calculated Using the Concentric Flow Model

Flow Rate (gpm)	Inlet Temp. (°C)	Wall Sat'n. Temp. Criterion Multiplier	Nominal Margin* (% of Power at Thermal Excursion)***	Margin with Uncertainties** (% of Power at Thermal Excursion)***
10	25	1.00	-3.3 to 2.0	24.6 to 28.4
		0.90	11.3 to 15.8	35.2 to 38.5
		0.878	14.5 to 18.9	37.6 to 40.8
		0.85	18.7 to 22.9	40.6 to 43.7
		0.80	26.0 to 29.8	46.0 to 48.8
10	40	1.00	-5.6 to -1.3	22.9 to 26.0
		0.90	12.1 to 15.7	35.8 to 38.4
		0.878	16.0 to 19.4	38.6 to 41.1
		0.85	20.9 to 24.2	42.2 to 44.6
		0.80	29.9 to 32.7	48.8 to 50.9
15	25	1.00	-2.4 to -0.4	25.2 to 26.7
		0.90	12.9 to 14.6	36.4 to 37.7
		0.878	16.2 to 17.9	38.8 to 40.0
		0.85	20.4 to 22.0	41.9 to 43.0
		0.80	27.8 to 29.3	43.0 to 47.3
15	40	1.00	-6.3 to -2.7	22.4 to 25.0
		0.90	12.5 to 15.5	36.1 to 38.3
		0.878	16.5 to 19.4	39.0 to 41.1.
		0.85	21.7 to 24.3	42.8 to 44.7
		0.80	30.7 to 33.1	49.4 to 51.1

*The nominal margin represents the margin between the measured power at the onset of thermal excursion and the limit calculated by FLOPA.

**The margin with uncertainties is the estimated margin between the measured power at the onset of thermal excursion and the estimated final limit after the application of uncertainties and biases in the LOPA limits analysis. This limit includes the effects of uncertainties in the heated length, the friction factor, the tube power fractions, the turbulent heat transfer coefficient, and tube thicknesses and a bias due to eccentrically located tubes. The nominal degree eccentricity allowed by rib tip clearances was used to compute this bias.

***The lower limit to the margin represents the margin between the highest measured power before the onset of thermal excursion and the calculated limit. The upper limit to the margin represents the margin between the measured power at thermal excursion and the calculated limit.

Table 8. Margins between Measured Thermal Excursion Powers and Wall Saturation Temperature Criterion Limits Calculated Using a Model with the Outer Channel Eccentricity Set to Match Calculated and Measured Differences between Hottest and Coldest Outer Channel Effluent Temperatures

Flow Rate (gpm)	Inlet Temp. (°C)	Wall Sat'n. Temp. Criterion Multiplier	Nominal Margin* (% of Power at Thermal Excursion)**
10	25	1.00	11.5 to 16.1
		0.90	16.9 to 21.2
		0.878	19.5 to 23.6
		0.85	22.8 to 26.8
		0.80	29.2 to 32.8
10	40	1.00	5.3 to 9.2
		0.90	17.6 to 21.0
		0.878	20.9 to 24.2
		0.85	25.1 to 28.2
		0.80	33.1 to 35.8
15	25	1.00	3.2 to 5.1
		0.90	16.8 to 18.5
		0.878	19.9 to 21.5
		0.85	23.8 to 25.3
		0.80	30.6 to 32.0
15	40	1.00	1.5 to 4.8
		0.90	18.0 to 20.8
		0.878	21.6 to 24.3
		0.85	26.3 to 28.8
		0.80	34.7 to 36.9

*The nominal margin represents the margin between the measured power at the onset of thermal excursion and the limit calculated by FLOPA, using a model in which the outer channel eccentricity is set to match measured and calculated differences between the hottest and coldest subchannel effluent temperatures.

**The lower limit to the margin represents the margin between the highest measured power before the onset of thermal excursion and the calculated limit. The upper limit to the margin represents the margin between the measured power at thermal excursion and the calculated limit.

Table 9. Wall Saturation Temperature Criterion Multipliers That Match Measured and Calculated Powers at Which the Maximum Wall Temperatures First Exceeded Saturation Temperatures, Based on Uncorrected Wall Temperature Measurements

Flow Rate (gpm)	Inlet Temperature (°C)	Power when Max. Wall Temp. = Satn. Temp. (kW)	Wall Saturation Temp. Criterion Multiplier
FLOPA Model with Concentric Flow Channels			
10	25	127.7	0.867
10	40	105.9	0.894
15	25	188.0	0.872
15	40	152.2	0.879
			0.878 = average
FLOPA Model with Outer Channel Eccentricity Set to Match Calculated and Measured Differences between Hottest and Coldest Outer Channel Effluent Temperatures			
10	25	127.7	0.906
10	40	105.9	0.936
15	25	188.0	0.898
15	40	152.2	0.910
			0.913 = average

Table 10. Wall Saturation Temperature Criterion Multipliers That Match Measured and Calculated Powers at Which the Maximum Wall Temperatures First Exceeded Saturation Temperatures, Based on Corrected Wall Temperature Measurements

Flow Rate (gpm)	Inlet Temperature (°C)	Power when Max. Wall Temp. = Satn. Temp. (kW)	Wall Saturation Temp. Criterion Multiplier
FLOPA Model with Concentric Flow Channels			
10	25	130.8	0.881
10	40	92.4	0.832
15	25	199.1	0.905
15	40	164.1	0.923
			0.885 = average
FLOPA Model with Outer Channel Eccentricity Set to Match Calculated and Measured Differences between Hottest and Coldest Outer Channel Effluent Temperatures			
10	25	130.8	0.924
10	40	92.4	0.856
15	25	199.1	0.933
15	40	164.1	0.950
			0.916 = average

Table 11. Variation of LOPA Limits with Wall Saturation Temperature Criterion Multiplier and Comparison with Current LOPA Stanton Number Limit

Wall Satn. Temp. Crit. Multiplier	Nominal Assembly Power (MW)	Percent of Historical Core Power	Best Est. Nominal Flow (gpm)	Stanton Number
Wall Saturation Temperature Limit*				
0.878	5.074	37	13.7	0.00150
Stanton Number Limit**				
----	5.686	41	13.0	0.00250

*The wall saturation temperature limit was computed using the LOPA transient for the K-14.1 subcycle with the wall saturation temperature criterion given in this report.

**The Stanton number limit was computed using a flow rate that is 70% of the best estimate flow rate from TRAC code calculations for Subcycle K-14.1 [1,7]. The limiting flow rate for subsequent reactor subcycles is expected to change.

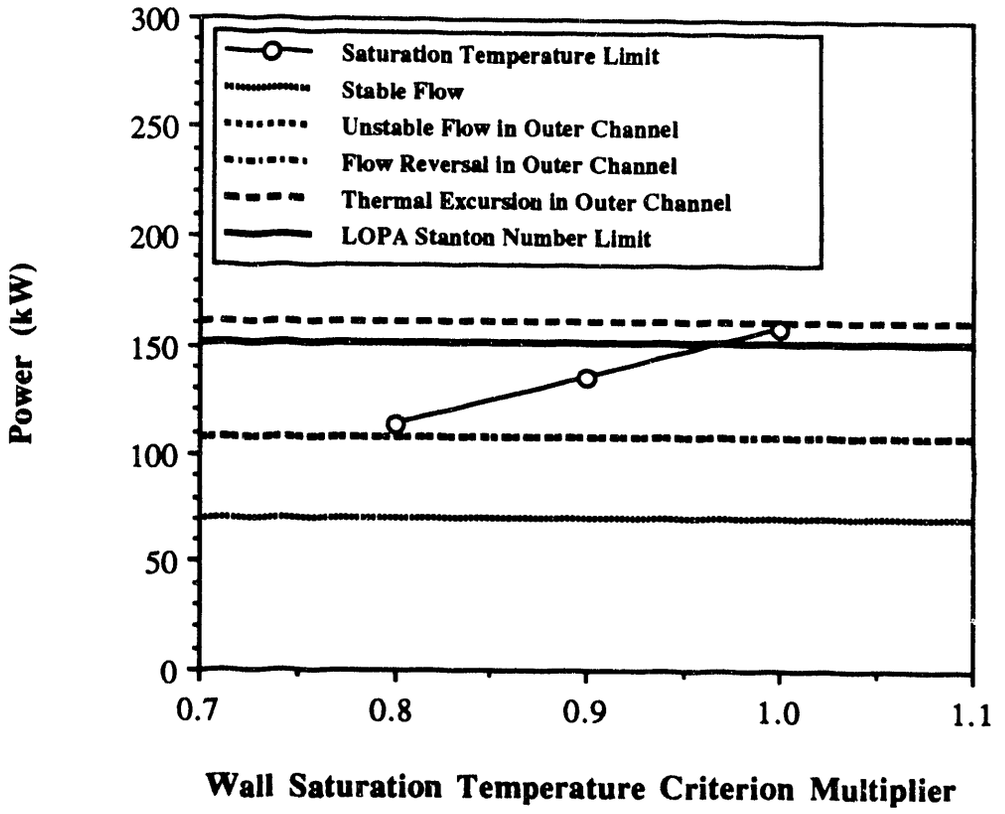

Figure 1. Comparison of Wall Saturation Temperature Criterion Limits with Measured Conditions for the SPRIHTE Tests at 10 gpm and 25°C Inlet, Using Concentric Flow Channels.

The wall temperature calculations used concentric channel dimensions.

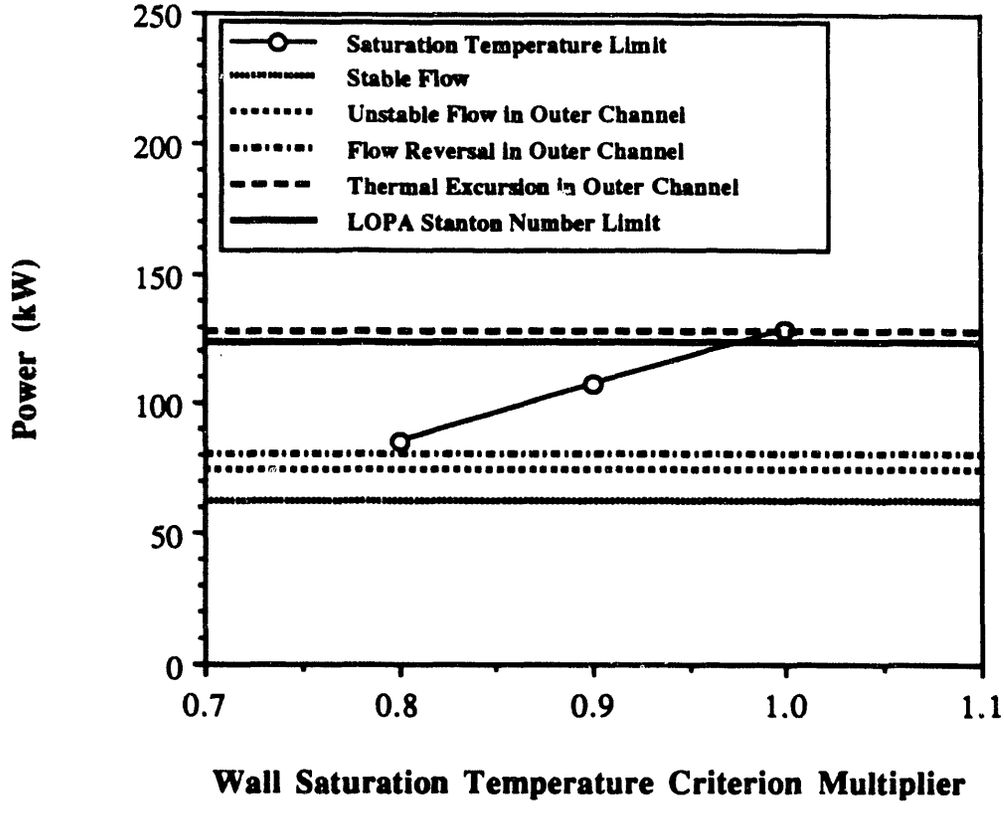

Figure 2. Comparison of Wall Saturation Temperature Criterion Limits with Measured Conditions for the SPRIHTE Tests at 10 gpm and 40°C Inlet, Using Concentric Flow Channels.

The wall temperature calculations used concentric channel dimensions.

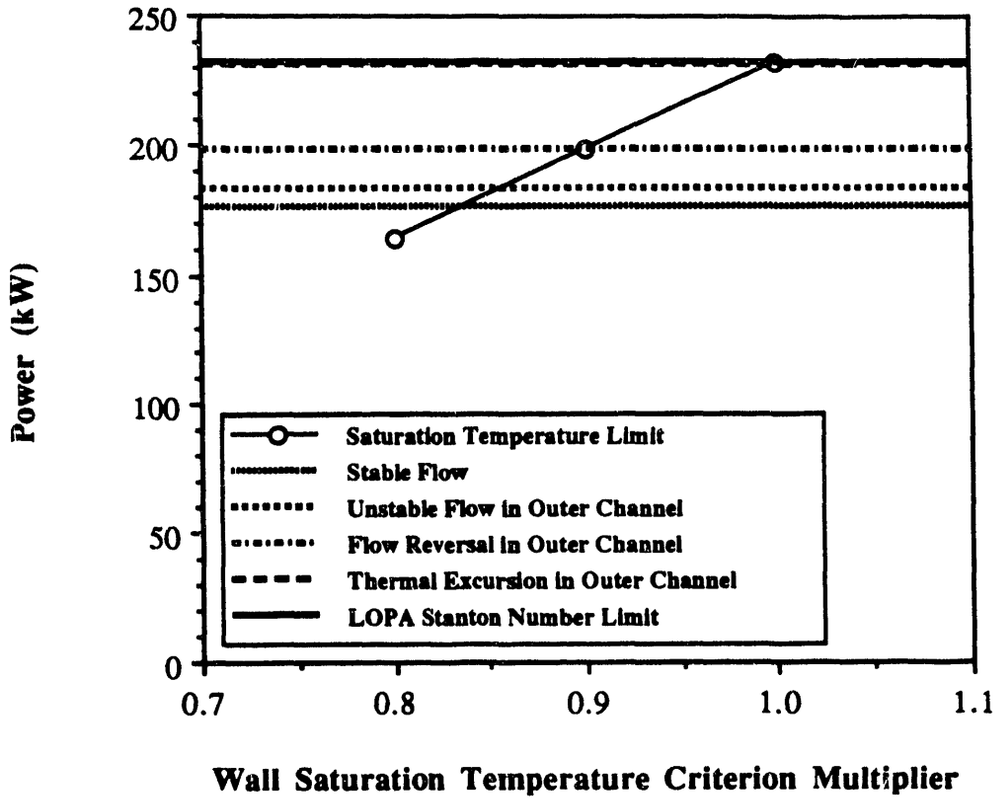

Figure 3. Comparison of Wall Satu ation Temperature Criterion Limits with Measured Conditions for the SPRIHTE Tests at 15 gpm and 25°C Inlet, Using Concentric Flow Channels.

The wall temperature calculations used concentric channel dimensions.

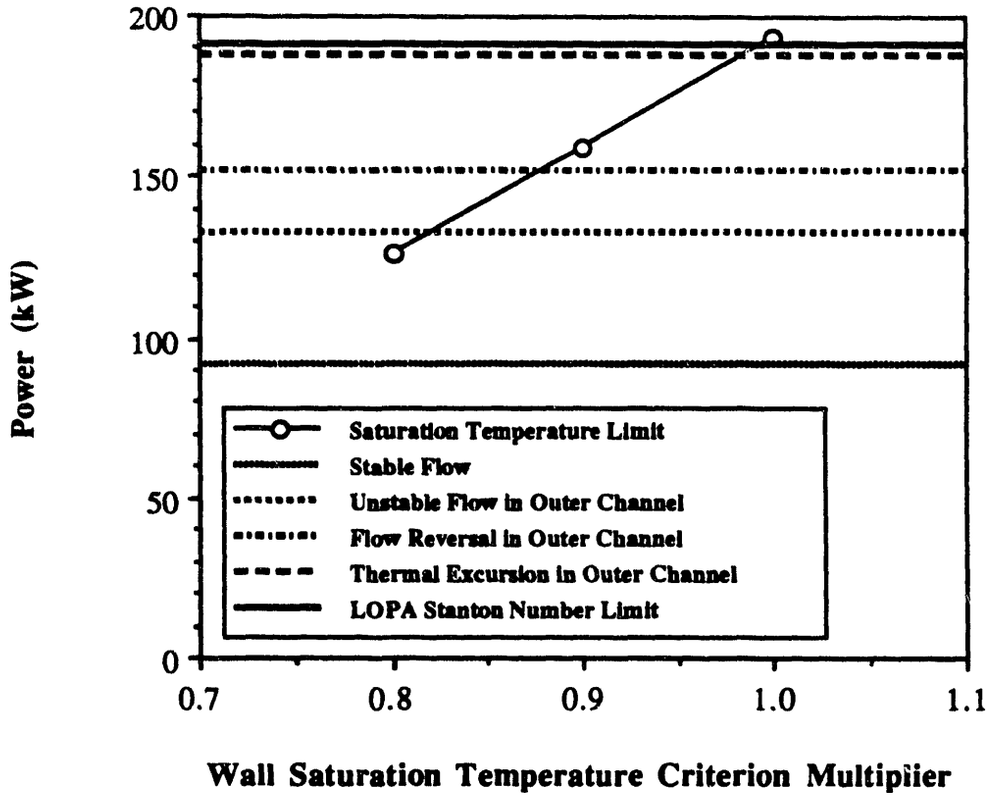

Figure 4. Comparison of Wall Saturation Temperature Criterion Limits with Measured Conditions for the SPRIHTE Tests at 15 gpm and 40°C Inlet, Using Concentric Flow Channels.

The wall temperature calculations used concentric channel dimensions.

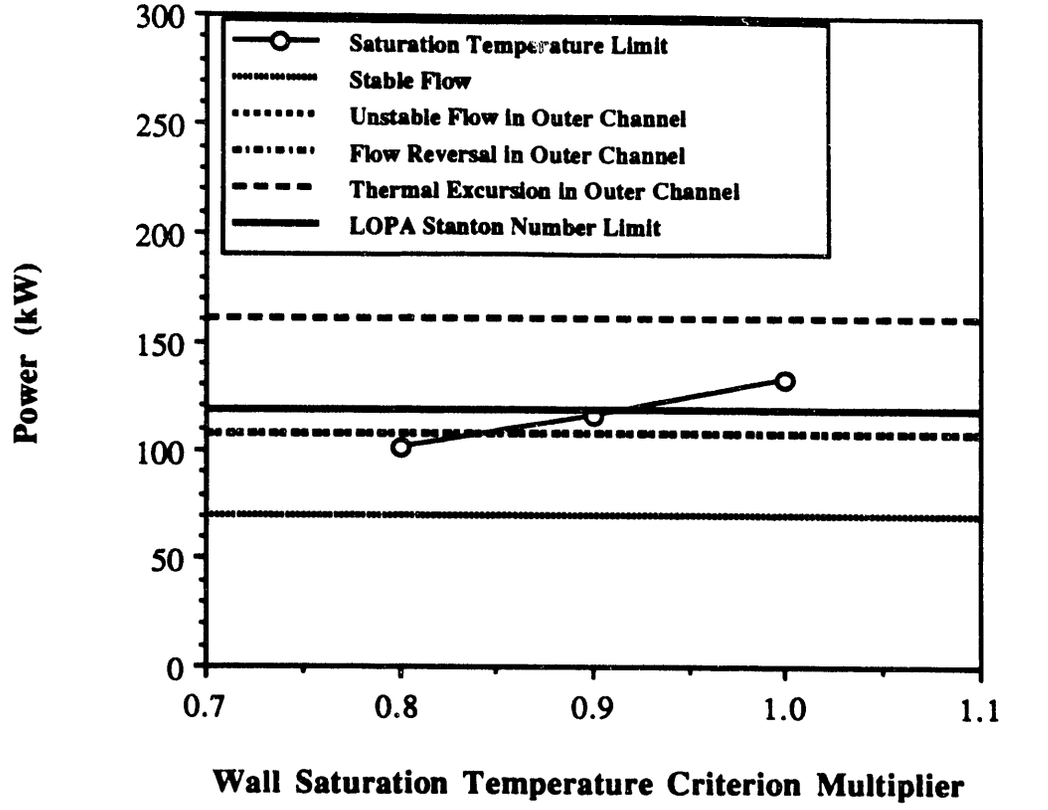

Figure 5. Comparison of Wall Saturation Temperature Criterion Limits with Measured Conditions for the SPRIHTE Tests at 10 gpm and 25°C Inlet, Using Nominal Eccentricity for the Outer Flow Channel.

The wall temperature calculations used the maximum allowable outer channel eccentricity based on the nominal rib tip clearance.

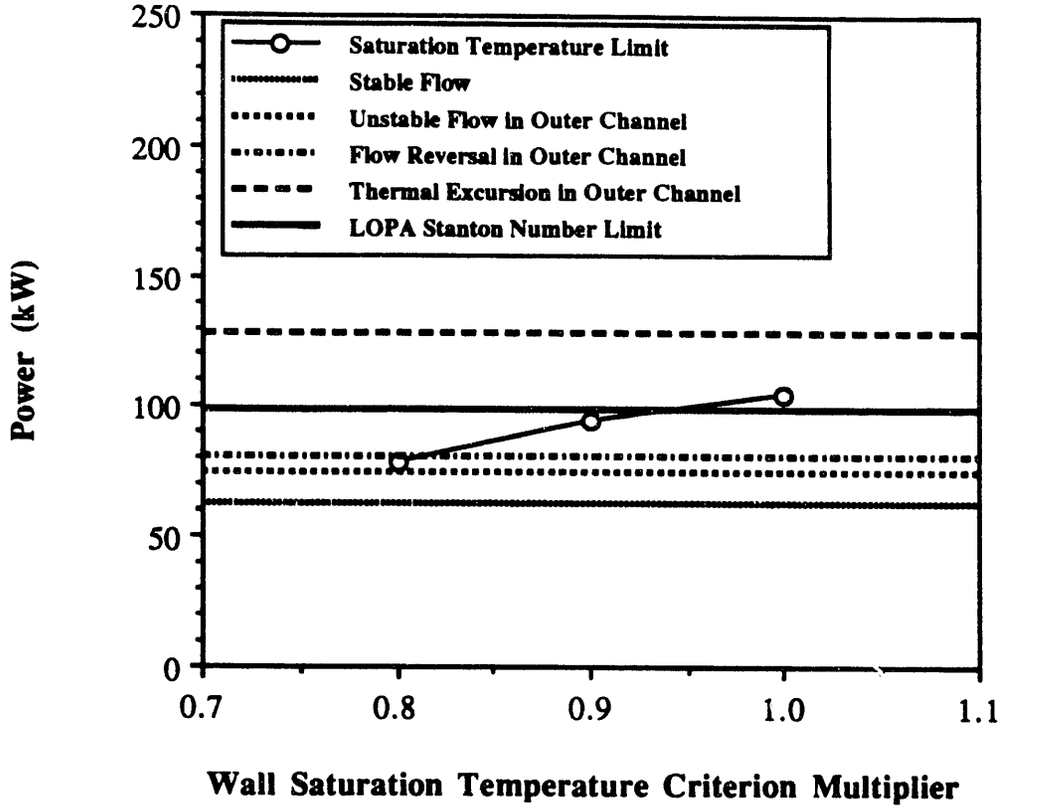

Figure 6. Comparison of Wall Saturation Temperature Criterion Limits with Measured Conditions for the SPRIHTE Tests at 10 gpm and 40°C Inlet, Using Nominal Eccentricity for the Outer Flow Channel.

The wall temperature calculations used the maximum allowable outer channel eccentricity based on the nominal rib tip clearance.

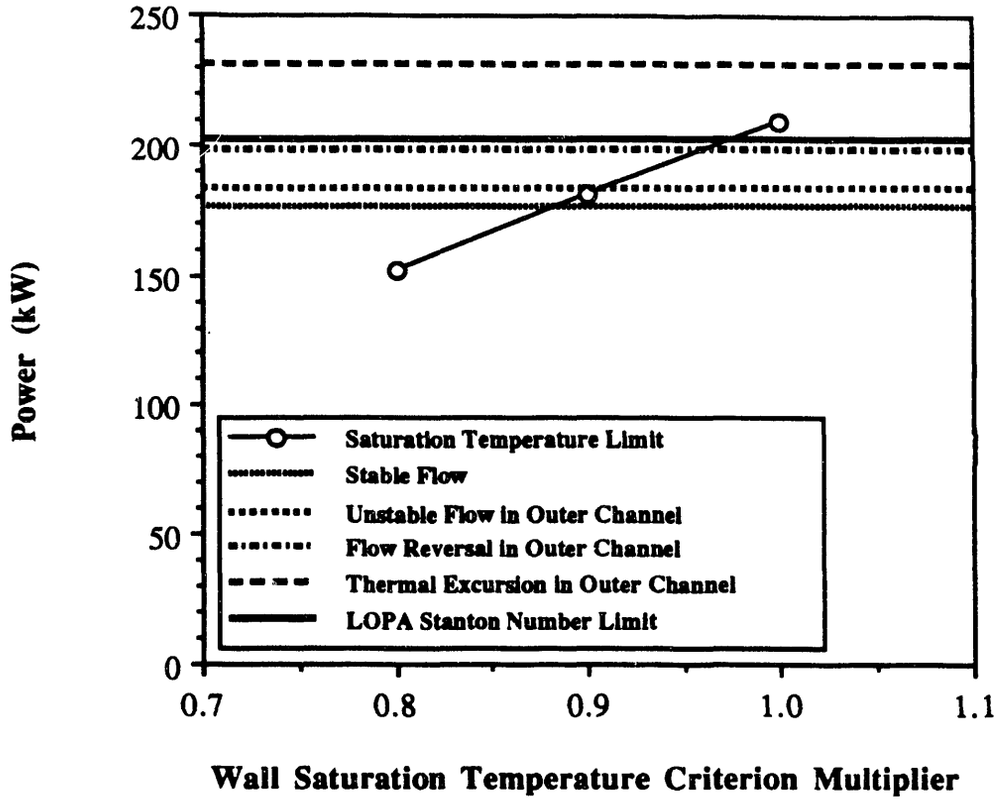

Figure 7. Comparison of Wall Saturation Temperature Criterion Limits with Measured Conditions for the SPRIHTE Tests at 15 gpm and 25°C Inlet, Using Nominal Eccentricity for the Outer Flow Channel.

The wall temperature calculations used the maximum allowable outer channel eccentricity based on the nominal rib tip clearance.

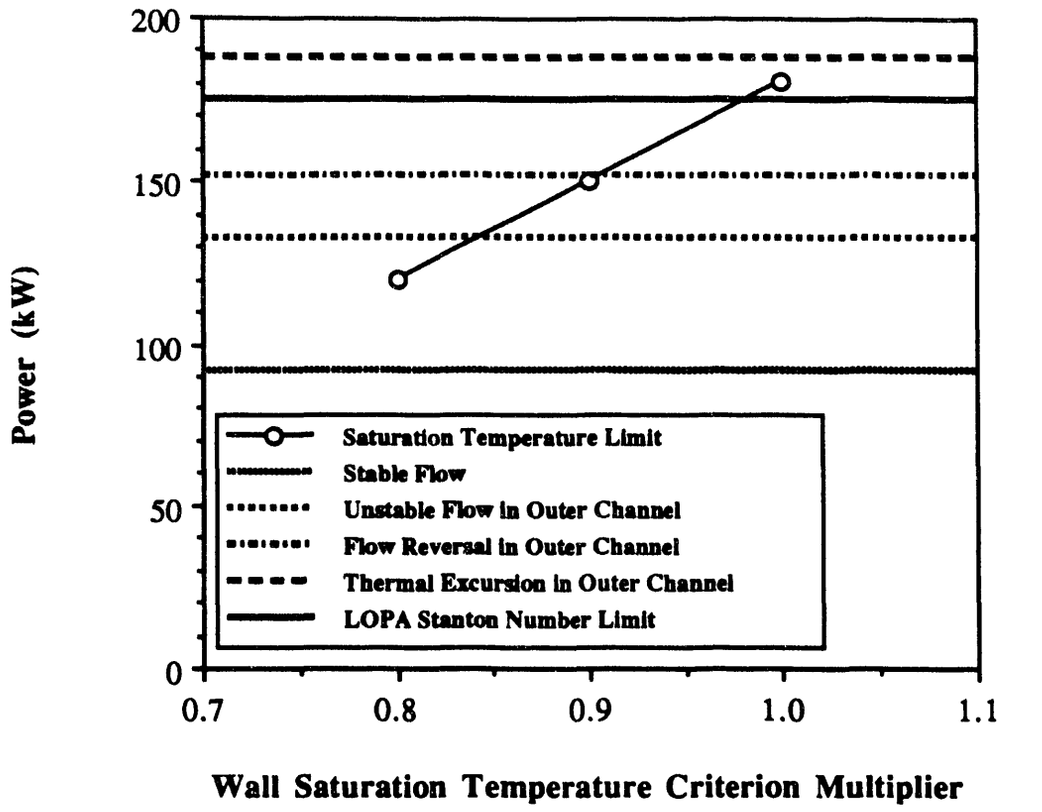

Figure 8. Comparison of Wall Saturation Temperature Criterion Limits with Measured Conditions for the SPRIHTE Tests at 15 gpm and 40°C Inlet, Using Nominal Eccentricity for the Outer Flow Channel.

The wall temperature calculations used the maximum allowable outer channel eccentricity based on the nominal rib tip clearance.

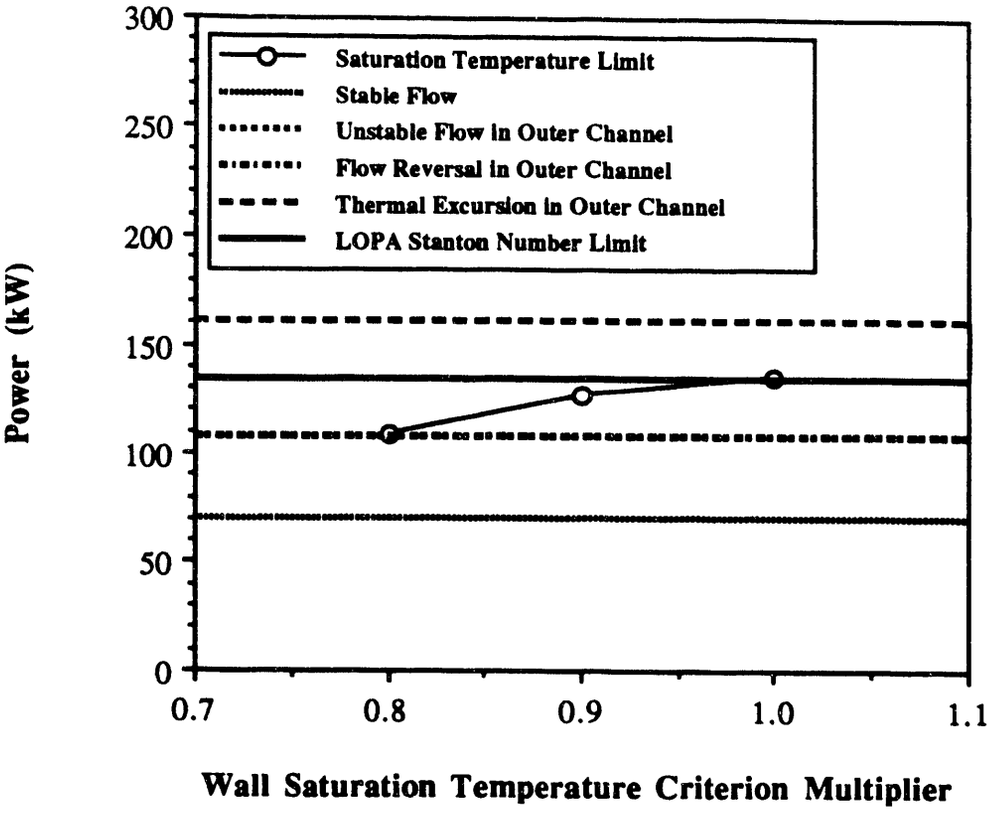

Figure 9. Comparison of Wall Saturation Temperature Criterion Limits with Measured Conditions for the SPRIHTE Tests at 10 gpm and 25°C Inlet, Using Estimated Eccentricity for the Outer Flow Channel.

In the wall temperature calculations, the outer channel eccentricity was set to match computed and measured values for the difference between the hottest and coldest subchannel effluent temperatures for the outer channel.

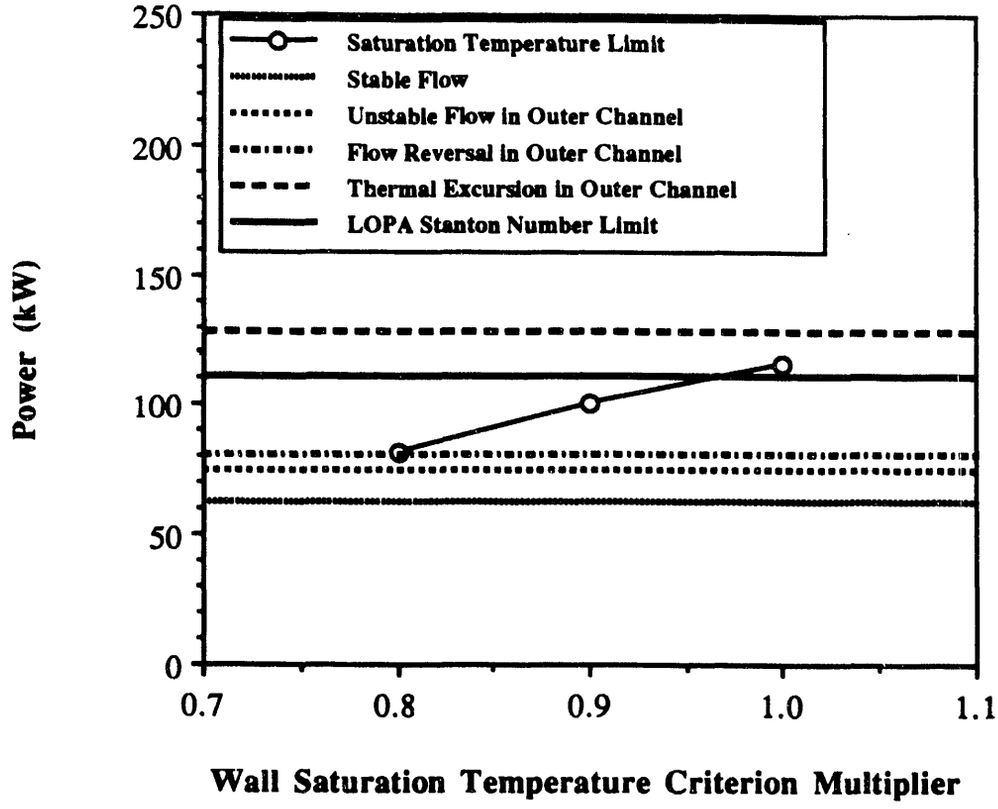

Figure 10. Comparison of Wall Saturation Temperature Criterion Limits with Measured Conditions for the SPRIHTE Tests at 10 gpm and 40°C Inlet, Using Estimated Eccentricity for the Outer Flow Channel.

In the wall temperature calculations, the outer channel eccentricity was set to match computed and measured values for the difference between the hottest and coldest subchannel effluent temperatures for the outer channel.

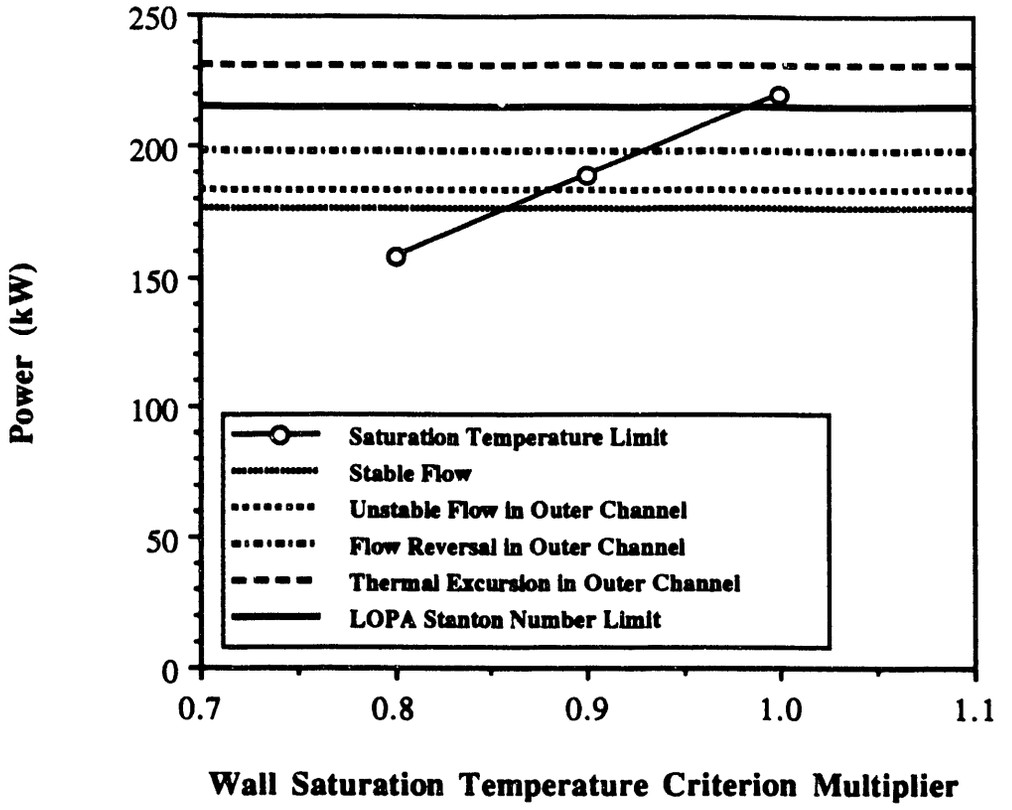

Figure 11. Comparison of Wall Saturation Temperature Criterion Limits with Measured Conditions for the SPRIHTE Tests at 15 gpm and 25°C Inlet, Using Estimated Eccentricity for the Outer Flow Channel.

In the wall temperature calculations, the outer channel eccentricity was set to match computed and measured values for the difference between the hottest and coldest subchannel effluent temperatures for the outer channel.

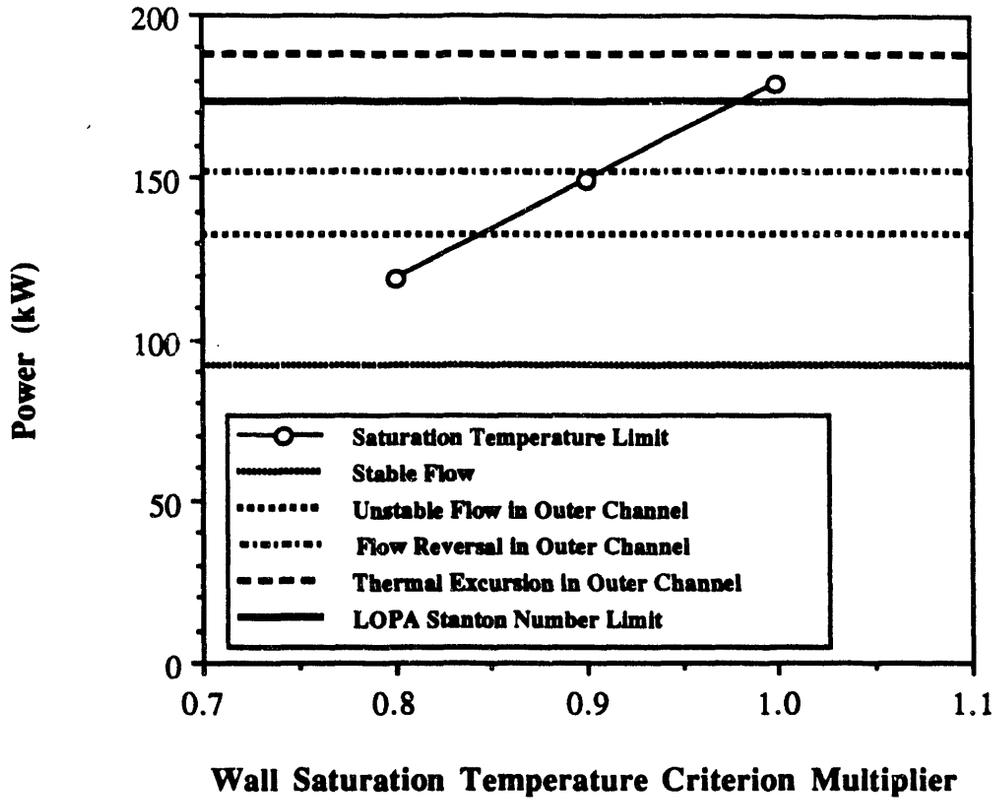

Figure 12. Comparison of Wall Saturation Temperature Criterion Limits with Measured Conditions for the SPRIHTE Tests at 15 gpm and 40°C Inlet, Using Estimated Eccentricity for the Outer Flow Channel.

In the wall temperature calculations, the outer channel eccentricity was set to match computed and measured values for the difference between the hottest and coldest subchannel effluent temperatures for the outer channel.

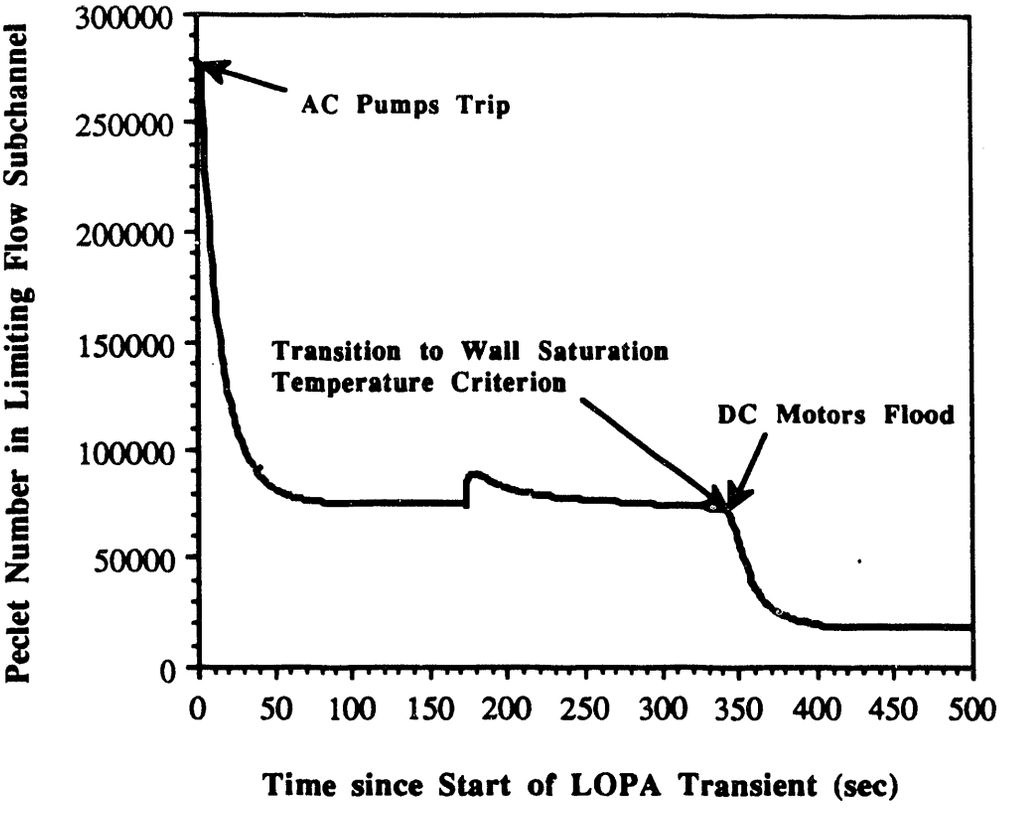

Figure 13. Variation of Peclet Numbers in the Limiting Subchannel during the Inlet Header Break LOPA Transient for Subcycle K-15.1.

Appendix A: Preparation of FLOPA Input for the Analysis of the SPRIHTE Tests

A.1 Description of FLOPA Model of SPRIHTE Rig

This appendix presents details of the preparation of the FLOPA input files for the analysis of the SPRIHTE tests and contains a sample input file. This input file is based on a standard input deck for a Mark 22 assembly for the K-14.1 subcycle [8].

The SPRIHTE test rig was constructed to be prototypic of a Mark 22 assembly. Therefore, Mark 22 dimensions were used to model the SPRIHTE rig. Small differences between Mark 22 design dimensions and the SPRIHTE as-built dimensions were ignored. Table A-1 lists these differences.

Table A-1. Comparison of Mark 22 Design and SPRIHTE Rig As-Built Dimensions

Dimension	Mark 22 Model	SPRIHTE Min.	SPRIHTE Max.
Inner Target OD	1.590	1.590	1.591
Inner Target Rib Circle	1.964	1.962	1.968
Inner Heater ID	1.995	1.991	1.994
Inner Heater OD	2.353	2.353	2.355
Inner Heater Rib Circle	2.863	2.860	2.867
Outer Heater ID	2.892	2.895	2.899
Outer Heater OD	3.200	3.203	3.205
Outer Target Rib Circle	3.230	3.227	3.245
Outer Target ID	3.540	3.525	3.543
Inner Heater Heated Length		148.0	
Outer Heater Heated Length		154.0	
Mark 22 Model Heater Overall Length		151.0	
Mark 22 Model Heater Heated Length		149.0	

SPRIHTE diametric dimensions are from Ref. [9]. SPRIHTE heated lengths are from Ref. [10]. All dimensions are in inches.

A.2 Differences between Mark 22 and SPRIHTE Rig Models

A list of changes made to the Mark 22 input file to model the SPRIHTE test rig follows.

1. The number of tubes was changed from 5 to 4. The USH and the outer purge channel were eliminated, since this purge channel is located in a separate pipe in the SPRIHTE rig. The small amount of flow in this purge channel (approximately 0.9% of the total flow) was ignored in the SPRIHTE analysis.

2. The axial power profile was calculated based on inner and outer heated relative flux measurements [10]. A spline function was used to compute the power profiles at 21 equally spaced intervals for each heater. The power profiles for the inner and outer heaters were averaged to come up with the input power profile. The program SPRSPLIN performed the spline interpolation, and the program SPRCOMB averaged the two spline fits. The inputs for SPRSPLIN for the outer and inner heater tubes, respectively, are SPRIHTE.DAT and SPRIHTE2.DAT, and the output files are SPRIHTE.OUT and SPRIHTE2.OUT. The output files for this program serve as the input files for

SPRCOMB. The output file for SPRCOMB is SPRIHTE3.OUT. Copies of the source code for SPRSPLIN and SPRCOMB and graphs that illustrate the results of the spline fit calculations are attached at the end of this appendix.

3. The SPRIHTE calculations were performed using the reactor assembly option for inputting form and friction pressure losses. This was done so that the inlet and bottom end fitting exit losses could be modeled accurately. Loss factors were obtained from the CMX hydraulic manual [11]. To get the FLOPA code to execute at elevated temperatures it was necessary to change the temperature basis for the loss factors from 17.5°C to either 45°C or 75°C. The following equations were used to calculate form and friction loss factors at these elevated temperatures.

$$c_{form} = c_{form,ref}\left(\frac{\rho}{\rho_{ref}}\right) \qquad \text{(A-1)}$$

$$c_{friction} = c_{friction,ref}\left(\frac{\rho}{\rho_{ref}}\right)^{0.8}\left(\frac{\mu}{\mu_{ref}}\right)^{0.2} \qquad \text{(A-2)}$$

where

c_{form} = form loss coefficient
$c_{form,ref}$ = form loss coefficient at reference temperature of hydraulics manual (17.5°C)
$c_{friction}$ = friction loss coefficient
$c_{friction,ref}$ = friction loss coefficient at reference temperature of hydraulics manual (17.5°C)
μ = fluid dynamic viscosity
μ_{ref} = fluid dynamic viscosity at reference temperature of hydraulics manual (17.5°C)
ρ = fluid density
ρ_{ref} = fluid density at reference temperature of hydraulics manual (17.5°C)

4. New cells were added at the top of the inlet section and at the bottom of the exit section to match the elevations of the plenum and tank bottom pressures in FLOPA with the measured elevations. The plenum pressure tap was 220.0±0.125 inches above the bottom of the heated section, and the tank bottom pressure tap was 17.8375±0.09375 inches below the bottom of the heated section [12]. The height of the top cell in the inlet section was adjusted to match the elevation of the middle of this cell to that of the plenum pressure tap. Likewise, the height of the bottom cell in the outlet section was adjusted to match the elevations of the middle of that cell and the tank bottom pressure tap.

5. The inlet section form loss was adjusted to match the calculated total assembly flow rate with the measured flow rate at the same pressure boundary conditions. This adjustment does not affect any result other than the plenum pressure for calculations with a fixed flow rate.

6. Three-dimensional, azimuthally asymmetric calculations were performed to determine when flow reversal would first occur in the outer flow channel. The measured differences among subchannel effluent temperatures were greatest in the outer channel; flow reversal and thermal excursions both started in this flow channel. Consequently, in the FLOPA calculations, it was assumed that only the outer flow channel was eccentric.

To model the eccentricity, cross-sectional areas, hydraulic diameters, and form and friction loss factors were adjusted for Subchannels 10 and 12 in the FLOPA input.

An initial set of calculations was performed with the maximum eccentricity allowed by rib tip clearances. (It was assumed that two adjacent ribs abutted against the outer housing. The limiting subchannel was located between these two ribs.) Subsequently, a second set of calculations was performed using an eccentricity that matched the calculated difference between the maximum and minimum subchannel effluent temperatures for the outer channel with the measured temperature difference. For each inlet temperature and flow rate, calculated and measured temperature differences were matched at the lowest power test condition, where the flow was stable. Finally, a set of calculations was performed using concentric flow channels. The concentric flow calculations were used to establish the LOPA limit criterion.

To model the subchannel eccentricities, subchannel areas, hydraulic diameters, and input form and heated section frictional loss coefficients were changed. Subchannel dimensions were obtained from a geometric analysis of rib clearances in a Mark 22 assembly [13]. The form and friction loss coefficients in the FLOPA code, which are defined in terms of pressure loss per unit volumetric flow, also change as the subchannel dimensions change. The following formulas were used to compute changes in the subchannel form and friction loss coefficients.

$$c_{form,min} = \left(\frac{D_{h,max}}{D_{h,min}}\right)^2 c_{form,max} \qquad \text{(A-3)}$$

$$c_{form,max} c_{form,min} = c^2_{form,avg} \qquad \text{(A-4)}$$

$$c_{friction,min} = \left(\frac{D_{h,max}}{D_{h,min}}\right)^3 c_{friction,max} \qquad \text{(A-5)}$$

$$c_{friction,max} c_{friction,min} = c^2_{friction,avg} \qquad \text{(A-6)}$$

where

$c_{form,avg}$ = average form loss coefficient for a subchannel in the outer channel
$c_{form,max}$ = maximum form loss coefficient for a subchannel in the outer channel
$c_{form,min}$ = minimum form loss coefficient for a subchannel in the outer channel
$c_{friction,avg}$ = average friction loss coefficient for a subchannel in the outer channel
$c_{friction,max}$ = maximum friction loss coefficient for a subchannel in the outer channel
$c_{friction,min}$ = minimum friction loss coefficient for a subchannel in the outer channel
$D_{h,avg}$ = average hydraulic diameter for a subchannel in the outer channel
$D_{h,max}$ = maximum hydraulic diameter for a subchannel in the outer channel, from Ref. [13]
$D_{h,min}$ = minimum hydraulic diameter for a subchannel in the outer channel, from Ref. [13]

The preceding equations can be derived based on the fact that, for an annular channel, the cross-sectional area is proportional to the hydraulic diameter.

In the calculations matching measured and calculated subchannel effluent temperatures, changes were performed iteratively until the computed span in effluent temperatures matched the measured span. The following formulas were used, along with Equations A-3 through A-6), to perform these iterations.

$$A_{max,update} = \frac{T_{max,meas} - T_{min,meas}}{T_{max,calc} - T_{min,calc}}\left(A_{max} - A_{avg}\right) + A_{avg} \qquad \text{(A-7)}$$

$$D_{h,max,update} = \frac{T_{max,meas} - T_{min,meas}}{T_{max,calc} - T_{min,calc}}\left(D_{h,max} - D_{h,avg}\right) + D_{h,avg} \qquad \text{(A-8)}$$

$$D_{h,min,update} = 2D_{h} - D_{h,max,update} \qquad \text{(A-9)}$$

$$A_{min,update} = 2A_{avg} - A_{max,update} \qquad \text{(A-10)}$$

where

A_{avg} = average cross-sectional area for a subchannel in the outer channel
A_{max} = previous estimate of maximum cross-sectional area for a subchannel in the outer channel
$A_{max,update}$ = updated estimate of maximum cross-sectional area for a subchannel in the outer channel
A_{min} = previous estimate of minimum cross-sectional area for a subchannel in the outer channel
$A_{min,update}$ = updated estimate of minimum cross-sectional area for a subchannel in the outer channel
$c_{form,avg}$ = average form loss coefficient for a subchannel in the outer channel
$c_{form,max}$ = maximum form loss coefficient for a subchannel in the outer channel
$c_{form,min}$ = minimum form loss coefficient for a subchannel in the outer channel
$c_{friction,avg}$ = average friction loss coefficient for a subchannel in the outer channel
$c_{friction,max}$ = maximum friction loss coefficient for a subchannel in the outer channel
$c_{friction,min}$ = minimum friction loss coefficient for a subchannel in the outer channel
$D_{h,avg}$ = average hydraulic diameter for a subchannel in the outer channel
$D_{h,max}$ = previous estimate of maximum hydraulic diameter for a subchannel in the outer channel
$D_{h,max,update}$ = updated estimate of maximum hydraulic diameter for a subchannel in the outer channel
$D_{h,min}$ = previous estimate of minimum hydraulic diameter for a subchannel in the outer channel
$D_{h,min,update}$ = updated estimate of maximum hydraulic diameter for a subchannel in the outer channel
$T_{max,calc}$ = maximum subchannel effluent temperature calculated by FLOPA
$T_{max,meas}$ = maximum measured subchannel effluent temperature
$T_{min,calc}$ = minimum subchannel effluent temperature calculated by FLOPA
$T_{min,meas}$ = minimum measured subchannel effluent temperature

The following two tables compare dimensions and loss factors for the eccentricities that match calculated and measured subchannel effluent temperature differences with nominal values and values calculated using maximum allowable rib tip clearances.

Table A-2. Subchannel Dimensions for Eccentric Models of the Outer Channel of the SPRIHTE Rig

Flow Rate (gpm)	T_{in} (°C)	A_{avg} (sqin)	A_{min} (sqin)	A_{max} (sqin)	$D_{h,avg}$ (in.)	$D_{h,min}$ (in.)	$D_{h,max}$ (in.)
Model Using Maximum Eccentricity Allowed by Rib Tip Clearances							
--------	--------	0.43975	0.39129	0.48821	0.319	0.28207	0.35415
Models Using Eccentricities That Match Measured and Calculated Subchannel Effluent Temperature Differences							
10	25	0.43975	0.41660	0.46290	0.319	0.30221	0.33579
10	40	0.43975	0.41602	0.46348	0.319	0.30179	0.33621
15	25	0.43975	0.42119	0.45831	0.319	0.30554	0.33246
15	40	0.43975	0.38321	0.49629	0.319	0.27799	0.36001

Table A-3. Subchannel Pressure Loss Factors for Eccentric Models of the Outer Channel of the SPRIHTE Rig

Flow Rate (gpm)	T_{in} (°C)	$C_{form,avg}$	$C_{form,min}$	$C_{form,max}$	$C_{friction,avg}$	$C_{friction,min}$	$C_{friction,max}$
		(psi/(100 gpm)²)			(psi/(100 gpm)²)		
Model Using Maximum Eccentricity Allowed by Rib Tip Clearances*							
10	25	6.4358	5.2216	8.1286	23.136	16.098	33.089
10	40	6.3372	5.1416	8.0041	20.868	15.250	29.845
15	25	6.4358	5.2216	8.1286	23.136	16.098	33.089
15	40	6.3372	5.1416	8.0041	20.868	15.250	29.845
Models Using Eccentricities That Match Measured and Calculated Subchannel Effluent Temperature Differences*							
10	25	6.4358	5.7921	7.1551	23.136	19.753	27.098
10	40	6.3372	5.6883	7.0602	20.868	17.746	24.539
15	25	6.4358	5.9145	7.0030	23.136	20.383	26.261
15	40	6.3372	4.8933	8.2072	20.868	14.159	30.756

* The form and friction loss coefficients for the tests at 25°C inlet are based on a reference temperature of 45°C. The coefficients for the tests at 40°C inlet are based on a reference temperature of 75°C.

A.3 Application of the FLOPA Model of the SPRIHTE Rig

The FLOPA model was used to calculate flow instability limits based on two criteria: 1) a Stanton number criterion (St = 0.0025) based on results of previous LOPA flow excursion tests conducted by B. S. Johnston in Rig FC, and 2) a wall saturation temperature criterion in which $T_{wall} = \beta T_{sat}$, where β is a multiplier that accounts for the inability of the model to accurately predict subchannel flow and heat transfer distributions. Limits were computed for four test conditions: 1) 10 gpm and 25°C inlet,

2) 10 gpm and 40°C inlet, 3) 15 gpm and 25°C inlet, and 4) 15 gpm and 40°C inlet. For each test condition, three sets of calculations were performed, one with concentric flow channel dimensions, a second with the maximum degree of eccentricity in the outer flow channel allowed by nominal rib tip clearances, and a third with an outer channel eccentricity set to match measured and calculated spreads in the outer subchannel effluent temperatures. These calculations used input conditions (inlet temperatures, flow rates, and outlet pressures) for the lowest power test for each combination of nominal flow rate and inlet temperature. Calculations were performed for β = 1.00, 0.90, 0.85, and 0.80.

A.4 Sample Input File for FLOPA Calculation of Flow Instability Limits for the SPRIHTE Tests

This input file uses a wall saturation temperature criterion with a multiplier of 0.85. The nominal inlet temperature is 25°C and the nominal flow rate is 10 gpm. The power limit for this calculation is 109.2 kW.

```
/MARK 22:k-14.1 Cell 18 2d test for axisymmetric 3d deck/
/RUN TIME SEC, NZONE, TMIN, TIME ZONE DATA/
 2000.      1    0.0
 3000.  1000.
/IPRTF, IPRTS, IPRTP, IDMPS, IBALN, ICRIT, IPRTSS, IPTIME, IPITER/
 1000   1000   1000     1
 10000   1000      0     1     0    0    0
/CRITERIA CHECKING FLAGS: ONB, TSAT, CHF, OSV, TMAX/
  0    0    0    0    1       0.0  5000.0
/TOLERANCES, ITERATIONS, AND INITIAL POWER/
 1.0D-03  10  0.107
 1.0D-06 600
 1.0D-03 600
/FLUID ITERATIONS, TOLERANCES, AND OPTIONS/
 1   1  1.0D-06
 1   1  1.0D-06
 1  1  1  2  1  1  1  0  0  2  0  0
 1
/POWER ARRAY PARAMETERS/
  5   3   0
  2   2   2   20   2    2    2    2    2    2    2
/SENSITIVITY MULTIPLIERS/
/MULTIPLIERS FOR METAL THERMAL CONDUCTIVITY/
 1.00  1.00  1.00  1.00  1.00  1.00  1.00  1.00  1.00
/MULTIPLIERS FOR METAL HEAT CAPAPCITY/
 1.00  1.00  1.00  1.00  1.00  1.00  1.00  1.00  1.00
/MULTIPLIERS FOR SINGLE PHASE HEAT TRANSFER CORRELATIONS/
 1.00  1.00  1.00  1.00  1.00
/MULTIPLIERS FOR FLUID PROPERTIES AND SUBCOOLED BOILING/
 1.00  1.00  1.00  1.00  1.00  1.00
/NULTIPLIERS THAT AFFECT ONSET OF NUCLEATE BOILING AND/
 1.00  1.00  1.00  1.00  1.00  1.00
/MA MCYLN ICENT AND NCELLS/
 8    4     0
 8   42    13
/RADIAL CELLS AND SUBCHANNELS/
 9  9  9  9
 1  4  4  4
/SURFACE CHECK FLAGS/
 0 0 0 1 1 1 1 0 0
/CYLINDER #1/
 1.0  1
  1  0.187   0.04250
 40  2  2  2  2  2  2  2  2  2
 1.235
 1.265
 1.295
 1.342
 1.389
 1.436
 1.483
 1.530
 1.560
 1.590
/CYLINDER #2/
 28.0  1
```

```
  1  0.255    0.03625
 40  2  2  2  2  2  2  2  2  2
 1.995
 2.025
 2.055
 2.103
 2.150
 2.198
 2.245
 2.293
 2.323
 2.353
/CYLINDER #3/
 28.0  1
  0     0.0     0.0
 40  2  2  2  2  2  2  2  2  2
 2.892
 2.922
 2.952
 2.990
 3.027
 3.065
 3.102
 3.140
 3.170
 3.200
/CYLINDER #4/
 1.0  1
 -1  0.155    0.03875
 40  2  2  2  2  2  2  2  2  2
 3.540
 3.570
 3.600
 3.608
 3.617
 3.625
 3.634
 3.642
 3.671
 3.700
/FLUID GEOMETRIC DATA SET/
 151.0     149.0  1.0  40.    1.0
  13.254     99.903
   0.10000
   0.05525  0.05525  0.05525  0.05525
   0.09000  0.09000  0.09000  0.09000
   0.07700  0.07700  0.07700  0.07700
   0.10000
   0.05525  0.05525  0.05525  0.05525
   0.09000  0.09000  0.09000  0.09000
   0.07700  0.07700  0.07700  0.07700
     1.198
   0.273      0.273     0.273     0.273
   0.539      0.539     0.539     0.539
   0.39129    0.43975   0.48821   0.43975
     1.235
   0.3522     0.3522    0.3522    0.3522
   0.4751     0.4751    0.4751    0.4751
   0.28207    0.319     0.35415   0.319
       0.0
       0.0      0.0       0.0       0.0
       0.0      0.0       0.0       0.0
       0.0      0.0       0.0       0.0
       0.0
```

```
       0.0       0.0       0.0       0.0
       0.0       0.0       0.0       0.0
       0.0       0.0       0.0       0.0
       0.0
       0.0       0.0       0.0       0.0
       0.0       0.0       0.0       0.0
       0.0       0.0       0.0       0.0
6.0000D-05
6.0000D-05  6.0000D-05  6.0000D-05  6.0000D-05
6.0000D-05  6.0000D-05  6.0000D-05  6.0000D-05
6.0000D-05  6.0000D-05  6.0000D-05  6.0000D-05
    0       15.905    13.254     0.0        0.000     0.
    0       26.508    13.254     2.00       0.0       0.
    1       90.459    13.254     0.0        1.000     0.
    1      109.956    13.254     8.75       0.0       0.
    2      141.372    12.566     0.0        1.000     0.
    2      172.788    12.566    13.75       0.0       0.
    3      151.550    12.566     0.0        1.000     0.
    3      130.313    12.566    10.37       0.0       0.
    4      144.827    12.566     0.0        1.000     0.
    4      159.342    12.566    12.68       0.0       0.
    5      123.101    11.781     0.0        1.000     0.
    5       71.476     7.839    10.50       0.0       0.
    6       60.571     4.832     0.0        1.000     0.
    6       65.052     7.839     9.75       0.0       0.
    7       39.570     8.884     0.0        1.000     0.
    7       17.768     8.884     2.00       0.0       0.
    1       17.768     8.884     2.00       0.0       0.
    1       13.959     8.884     0.0        1.000     0.
    2       10.149     8.982     1.13       0.0       0.
    2        7.406     9.079     0.0        1.000     0.
    3        4.663     7.174     0.65       0.0       0.
    3        3.697     5.268     0.0        1.000     0.
    4        2.731     5.462     0.50       0.0       0.
    4        4.513     5.656     0.0        1.000     0.
    5        6.295     5.995     1.05       0.0       0.
    5        5.789     6.334     0.0        1.000     0.
    6        5.283     6.604     0.80       0.0       0.
    6        2.961     2.553     0.0        1.000     0.
    7        0.638     2.553     0.25       0.0       0.
    7        3.287     2.553     0.0        1.000     0.
    8        5.935     7.419     0.80       0.0       0.
    8        5.750     7.419     0.0        1.000     0.
    9        5.564     7.419     0.75       0.0       0.
    9        8.532     7.419     0.0        1.000     0.
   10       11.499     7.419     1.55       0.0       0.
   10       15.580     7.419     0.0        1.000     0.
   11       19.660     7.419     2.65       0.0       0.
   11       10.004     1.391     0.0        1.000     0.
   12        0.348     1.391     0.25       0.0       0.
   12        6.600     1.391     0.0        1.000     0.
   13        2.782   200.000     2.00       0.0       0.
   13      699.000   200.000     0.0        1.000     0.
      1.0
      1.5       1.5       1.5       1.5
      1.5       1.5       1.5       1.5
      1.5       1.5       1.5       1.5
      0.14
/ASSEMBLY EXPOSURE/
 0.0 0 0.0 0.0
/14. POWER FRACTIONS MEASURED/
 4 1
0.0 0.0 0.0 0.0
0.39205 0.0 0.0 0.0
```

```
         0.60795 0.0 0.0 0.0
           0.0 0.0 0.0 0.0
/15. RADIAL SHAPES/
 4 3 3
 1 0 0 0 0
 1.0 0.0 0.0
 1.0 0.0 0.0
 1.0 0.0 0.0
 2 0 0 0 0
 1.0 0.0 0.0
 1.0 0.0 0.0
 1.0 0.0 0.0
 3 0 0 0 0
 1.0 0.0 0.0
 1.0 0.0 0.0
 1.0 0.0 0.0
 4 0 0 0 0
 1.0 0.0 0.0
 1.0 0.0 0.0
 1.0 0.0 0.0
/WET TANK SHAPE POWER FRACTIONS/
 0
/DRY TANK SHAPE POWER FRACTIONS/
 0
 /16. AZIMUTHAL SHAPES /
     4   8  13
      1  0  0  0  0
      2  0  0  0  0
      3  0  0  0  0
      4  0  0  0  0
     1.0   1.0   1.0   1.0
     1.0   1.0   1.0   1.0
     1.0   1.0   1.0   1.0
     1.0   1.0   1.0   1.0
     1.0   1.0   1.0   1.0
     1.0   1.0   1.0   1.0
     1.0   1.0   1.0   1.0
     1.0   1.0   1.0   1.0
     1.0
     1.0   1.0   1.0   1.0
     1.0   1.0   1.0   1.0
     1.0   1.0   1.0   1.0
/FISSION POWER/
 3
       0.0  1.0000
1000.0   1.0000
2000.0   1.0000
/MODERDATED DECAY/
 3
       0.0  1.0000
1000.0   1.0000
2000.0   1.0000
/19. DRY DECAYH RESPONS/
 3
       0.0  1.0000
1000.0   1.0000
2000.0   1.0000
/20. AXIAL POWR RESPONS WORST COS 9-88/
 21 3
0.0 1000.0 10000.0
   0.00000   0.47204
   0.05000   0.52057
   0.10000   0.66783
   0.15000   0.77473
```

```
   0.20000   0.89176
   0.25000   0.99628
   0.30000   1.09984
   0.35000   1.19759
   0.40000   1.28723
   0.45000   1.35297
   0.50000   1.41304
   0.55000   1.43166
   0.60000   1.41112
   0.65000   1.35347
   0.70000   1.26365
   0.75000   1.14661
   0.80000   0.98242
   0.85000   0.81346
   0.90000   0.60535
   0.95000   0.46876
   1.00000   0.47151
   0.47204
   0.52057
   0.66783
   0.77473
   0.89176
   0.99628
   1.09984
   1.19759
   1.28723
   1.35297
   1.41304
   1.43166
   1.41112
   1.35347
   1.26365
   1.14661
   0.98242
   0.81346
   0.60535
   0.46876
   0.47151
   0.47204
   0.52057
   0.66783
   0.77473
   0.89176
   0.99628
   1.09984
   1.19759
   1.28723
   1.35297
   1.41304
   1.43166
   1.41112
   1.35347
   1.26365
   1.14661
   0.98242
   0.81346
   0.60535
   0.46876
   0.47151
/21. INLET FLOW/
   3
0.000 10.120
1000.000 10.120
2000.000 10.120
```

```
/tank bottom pressure transient for cell 15/
   3
0.000 23.698
1000.000 23.698
2000.000 23.698
/ASS TINLET TRANSIENT/
   3
0.000 26.404
1000.000 26.404
2000.000 26.404
/TANK LEVEL TRANSIENT/
       3
        0.0         1.0000
     1000.0         1.0000
     2000.0         1.0000
/FLUID INITIAL GUESS DATA/
  0.0050
  0.0530   0.0530   0.0530   0.0530
  0.1200   0.1200   0.1200   0.1200
  0.0632   0.0757   0.0884   0.0757
 303.00000  79.69575  45. 0.
  0.001900
  0.045800 0.045800 0.045800 0.045800
  0.126350 0.126350 0.126350 0.126350
  0.077375 0.077375 0.077375 0.077375
  1.0D0     1.0D0     1.0D0
  0.0     45.0      19.7
 3.937D-05  1.0  1.0   1.0   0.3846   0.85
/MK22  MANUAL LOSS COEFFICIENTS/
/REFERENCE TEMPS (TOP,MID,BOT)/
 45.0    45.0    45.0
/TOP SECTION MANUAL FORM LOSS COEFFICIENTS/
  0    0.0     0     0
  1    1.77    0     3
  2    0.0     0     0
  3    0.0     0     0
  4    0.0     3     4
  5    0.000   4     7
  6    0.0     0     0
  7    0.0     0     0
/MIDDLE SECTION (CHANNEL ENTRANCE) MANUAL FORM LOSS COEFFICIENTS/
  1 111302.0          7
  2      8.7108       7
  3      8.7108       7
  4      8.7108       7
  5      8.7108       7
  6      2.3823       7
  7      2.3823       7
  8      2.3823       7
  9      2.3823       7
 10      8.1286       7
 11      6.4358       7
 12      5.2216       7
 13      6.4348       7
/MIDDLE SECTION (CHANNEL LENGTH) MANUAL FRICTIONAL LOSS COEFFICIENTS/
  1   0.0
  2  47.978
  3  47.978
  4  47.978
  5  47.978
  6   9.847
  7   9.847
  8   9.847
  9   9.847
```

```
 10  33.089
 11  23.136
 12  16.908
 13  23.136
/MIDDLE SECTION (CHANNEL EXIT) MANUAL FORM LOSS COEFFICIENTS/
  1         0.0           4
  2         0.5396        4
  3         0.5396        4
  4         0.5396        4
  5         0.5396        4
  6         0.5298        4
  7         0.5298        4
  8         0.5298        4
  9         0.5298        4
 10         0.3836        4
 11         0.3836        4
 12         0.3836        4
 13         0.3836        4
/BOTTOM SECTION MANUAL FORM LOSS COEFFICIENTS/
  1    0.0      0     0
  2    0.0      0     0
  3    0.0      0     0
  4    0.0      0     0
  5    0.0      0     0
  6    1.016    4     8
  7    0.0      0     0
  8    0.0      0     0
  9    0.0      0     0
 10    0.0      0     0
 11    0.0      8    13
 12    0.0      0     0
 13    0.0      0     0
/AUXILIARY ORIFICE INFORMATION/
  0    0.0000   4
  1
     0.0    0.0
/BEF SHELL HOLE INFORMATION/
  0   36   0.3557   11
  5
  3.493    0.
-15.86     1.
 31.97     2.
-32.41     3.
 12.96     4.
/INITIAL SOLID TEMPERATURES/
 45.  45.
```

A.5 Source Listing for SPRSPLIN

```
c This program prepares tabulated axial power shape profiles for FLOPA input
c files.  The program was written to be used in the benchmarking of the
c SPRIHTE FLOPA flow excursion tests.  To run this program prepare an input
c file (File #5) containing paired data giving the axial location as a fraction
c of the distance down the heated section (x) and the ratio of the local power
c to the average power for the heated section (y).  The program uses a spline
c fit algorithm to calculate local powers (y1) at 21 evenly spaced locations
c (x1).  This output is written to File #6.
c
      program sprsplin
      dimension x(100),y(100),y2(100),y3(21)
      ni=0
      do 1 i=1,100
      read(5,*,end=99) x(i),y(i)
      x(i)=x(i)/149.0
      ni=ni+1
    1 continue
   99 continue
      call spline (x,y,ni,y2)
      do 2 i=1,21
      x1=0.05*float(i-1)
      call splint (x,y,y2,ni,x1,y1)
      write(6,101) x1,y1
      y3(i)=y1
    2 continue
      do 3 i=1,21
      write(6,102) y3(i)
    3 continue
  101 format (2(2x,f8.5))
  102 format (2x,f8.5)
      stop
      end
c
c The following two subroutines calculate a spline fit based on the measured
c input data and apply this fit to interpolate for a calculated power profile.
c These subroutines are adapted from pages 86-89 of Numerical Recipes:  The Art
c of Scientific Computing, by W. H. Press et al.  The subroutine spline has
c been modified to automatically apply natural end conditions (zero second
c derivatives at either end).  The calculations to interpolate among tabulated
c axial positions was changed in subroutine splint.
c
      subroutine spline (x,y,n,y2)
      parameter (nmax=100)
      dimension x(n),y(n),y2(n),u(nmax)
      y2(1)=0.
      u(1)=0.
      do 11 i=2,n-1
      sig=(x(i)-x(i-1))/(x(i+1)-x(i-1))
      p=sig*y2(i-1)+2.
      y2(i)=(sig-1.)/p
      u(i)=(6.*((y(i+1)-y(i))/(x(i+1)-x(i))-(y(i)-y(i-1))
     1/(x(i)-x(i-1)))/(x(i+1)-x(i-1))-sig*u(i-1))/p
   11 continue
      y2(n)=0.
      do 12 k=n-1,1,-1
      y2(k)=y2(k)*y2(k+1)+u(k)
   12 continue
      return
      end
c
```

```
      subroutine splint (xa,ya,y2a,n,x,y)
      dimension xa(n),ya(n),y2a(n)
      do 1 k=1,n-1
      if (xa(k).le.x.and.xa(k+1).ge.x) then
      klo=k
      khi=k+1
      end if
    1 continue
      h=xa(khi)-xa(klo)
      a=(xa(khi)-x)/h
      b=(x-xa(klo))/h
      y=a*ya(klo)+b*ya(khi)+
     1((a**3-a)*y2a(klo)+(b**3-b)*y2a(khi))*h**2/6.
      return
      end
```

A.6 Source Listing for SPRCOMB

```
c This program averages tabulated axial power shape profiles for FLOPA input
c files.  The program was written to be used in the benchmarking of the
c SPRIHTE LOPA flow excursion tests.  To run this program obtain input files
c (Files #4 and 5) by running the SPRSPLIN code.  These input files contain
c paired data giving the axial location as a fraction of the distance down the
c heated section (x) and the ratio of the local power to the average power for
c the heated section (y).  The output (in File #6) consists of the same data
c averaged for the two heater tubes.
c
      program sprcomb
      dimension x(21),y1(21),y2(21),y3(21)
      do 1 i=1,21
      read(4,*) x(i),y1(i)
      read(5,*) x(i),y2(i)
      y3(i)=0.5*(y1(i)+y2(i))
    1 continue
      do 2 i=1,21
      write(6,101) x(i),y3(i)
    2 continue
      do 3 i=1,21
      write(6,102) y3(i)
    3 continue
  101 format (2(2x,f8.5))
  102 format (2x,f8.5)
      stop
      end
```

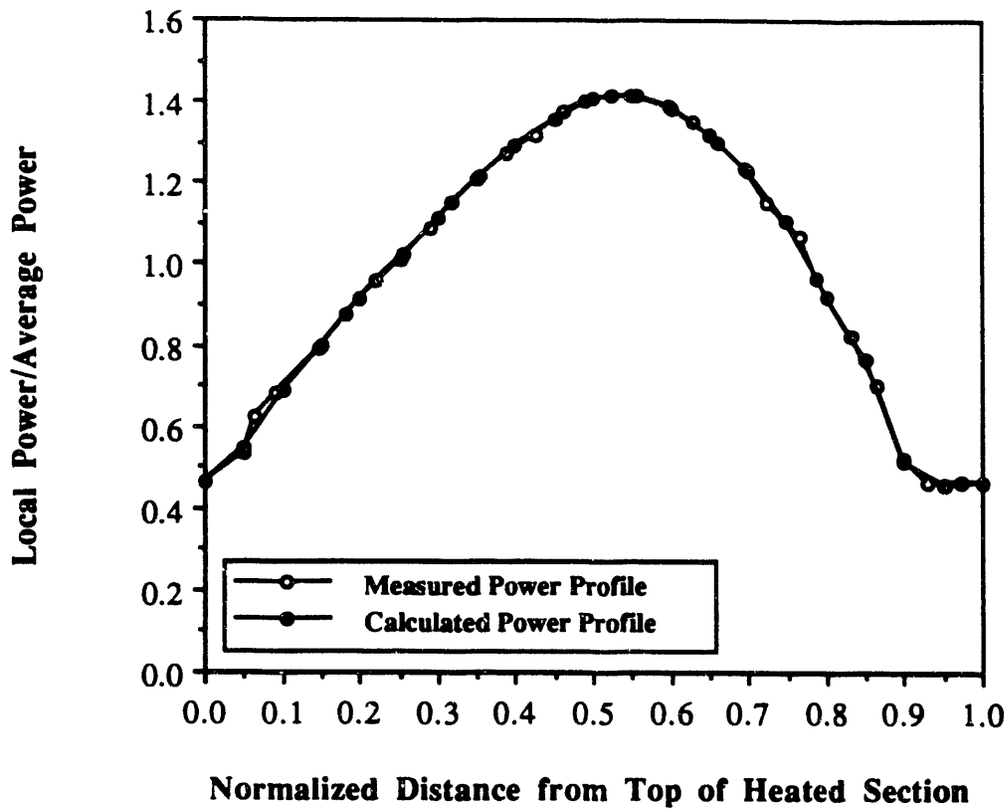

Figure A-1. Comparison of Measured Power Profile for the Outer Heater Tube with the Spline Fit Calculated by SPRSPLIN.

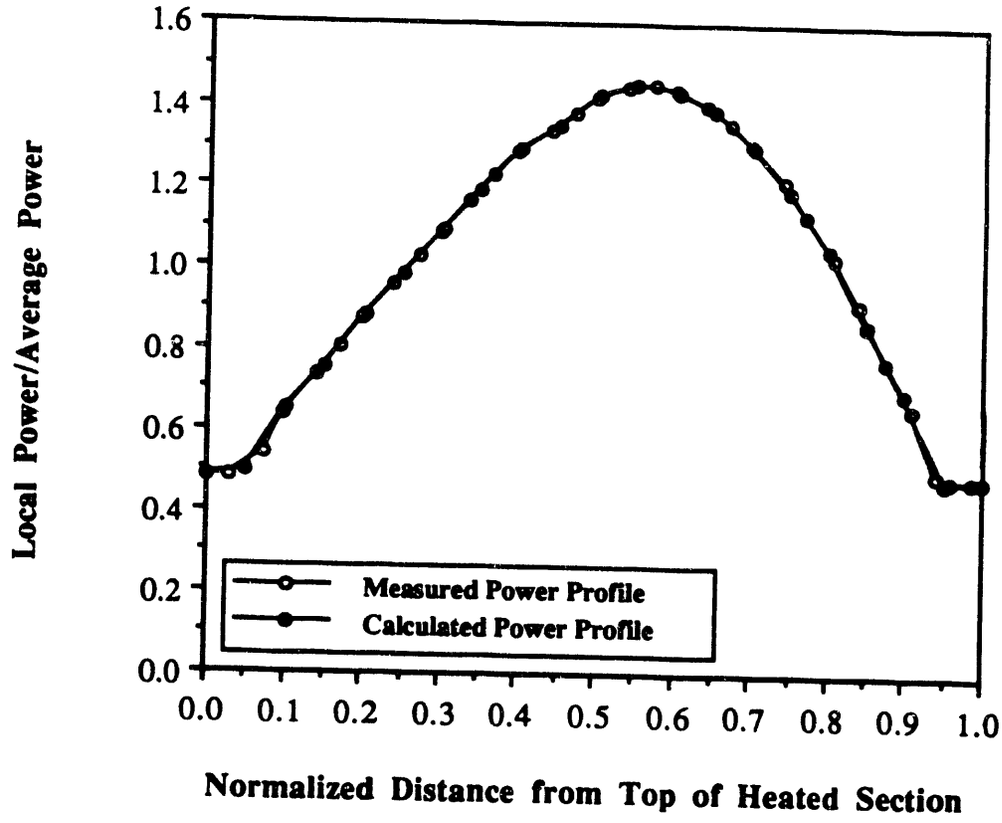

Figure A-2. Comparison of Measured Power Profile for the Inner Heater Tube with the Spline Fit Calculated by SPRSPLIN.

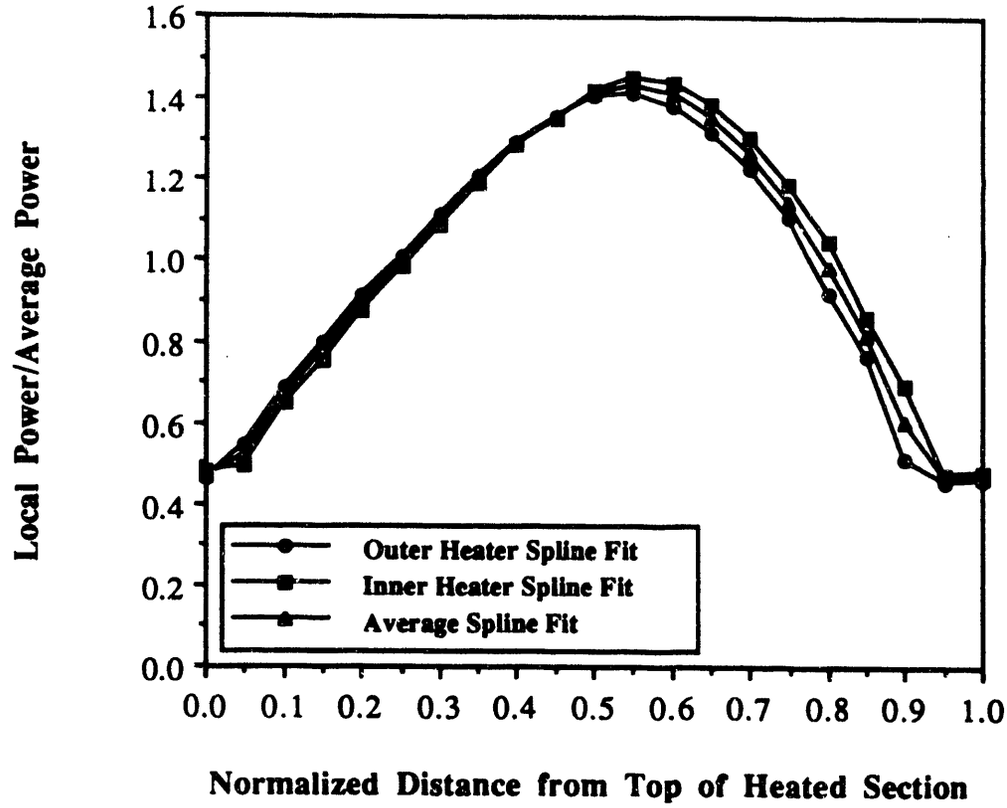

Figure A-3. Comparison of the Average Power Profile Calculated by SPRCOMB with Spline Fits for the Outer and Inner Heater Tubes.

Appendix B: Comparisons of Measured and Calculated Bulk Fluid Temperatures

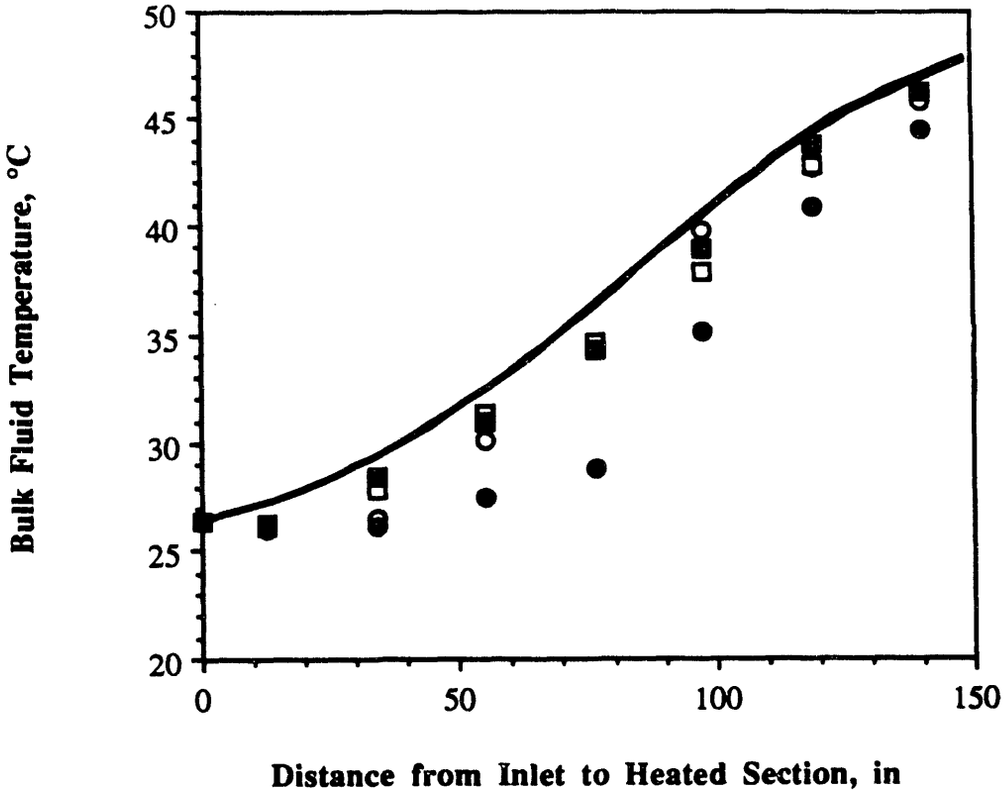

Figure B-1. Comparison of Measured and Calculated Subchannel Fluid Temperatures for the Inner Channel for the SPRIHTE Test at 10 gpm, 25°C Inlet, and 70 kW.

Symbols represent inner channel fluid temperature measurements for the four subchannels. Lines represent calculated inner channel fluid temperatures for the four subchannels. (Calculated temperature profiles for two or more subchannels may coincide because of assumed symmetries in the model.) No correspondence between calculated temperature profiles and specific subchannel measurements is implied.

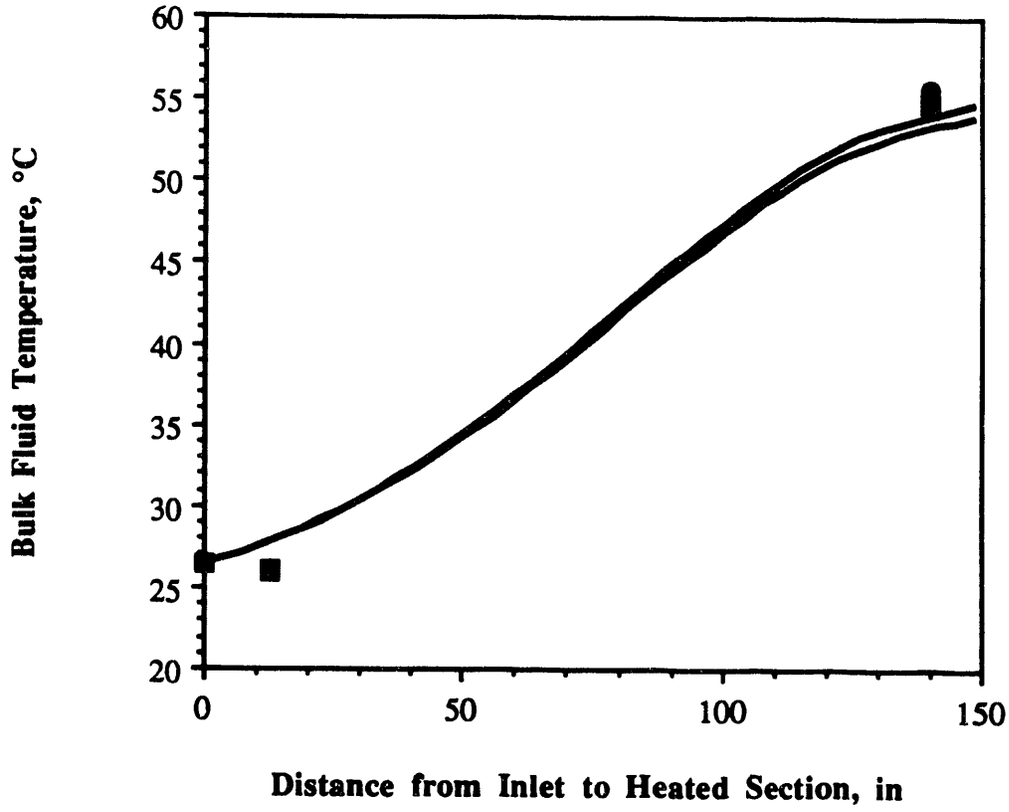

Figure B-2. Comparison of Measured and Calculated Subchannel Fluid Temperatures for the Middle Channel for the SPRIHTE Test at 10 gpm, 25°C Inlet, and 70 kW.

Symbols represent middle channel fluid temperature measurements for the four subchannels. Lines represent calculated middle channel fluid temperatures for the four subchannels. (Calculated temperature profiles for two or more subchannels may coincide because of assumed symmetries in the model.) No correspondence between calculated temperature profiles and specific subchannel measurements is implied.

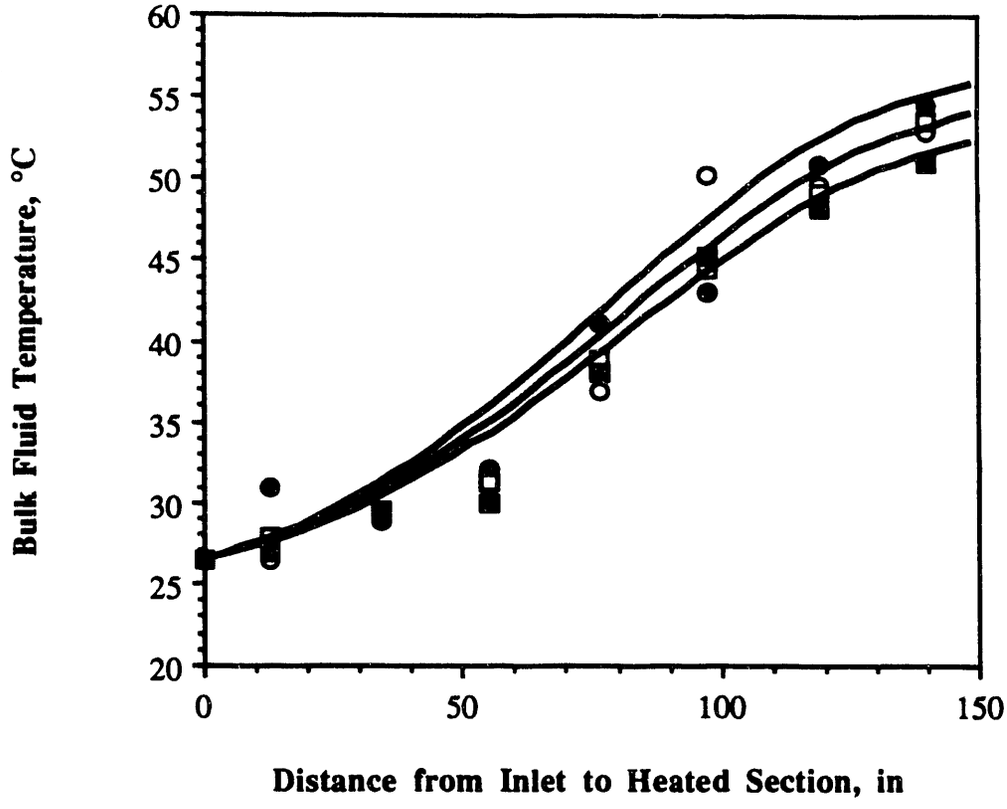

Figure B-3. Comparison of Measured and Calculated Subchannel Fluid Temperatures for the Outer Channel for the SPRIHTE Test at 10 gpm, 25°C Inlet, and 70 kW.

Symbols represent outer channel fluid temperature measurements for the four subchannels. Lines represent calculated outer channel fluid temperatures for the four subchannels. (Calculated temperature profiles for two or more subchannels may coincide because of assumed symmetries in the model.) No correspondence between calculated temperature profiles and specific subchannel measurements is implied.

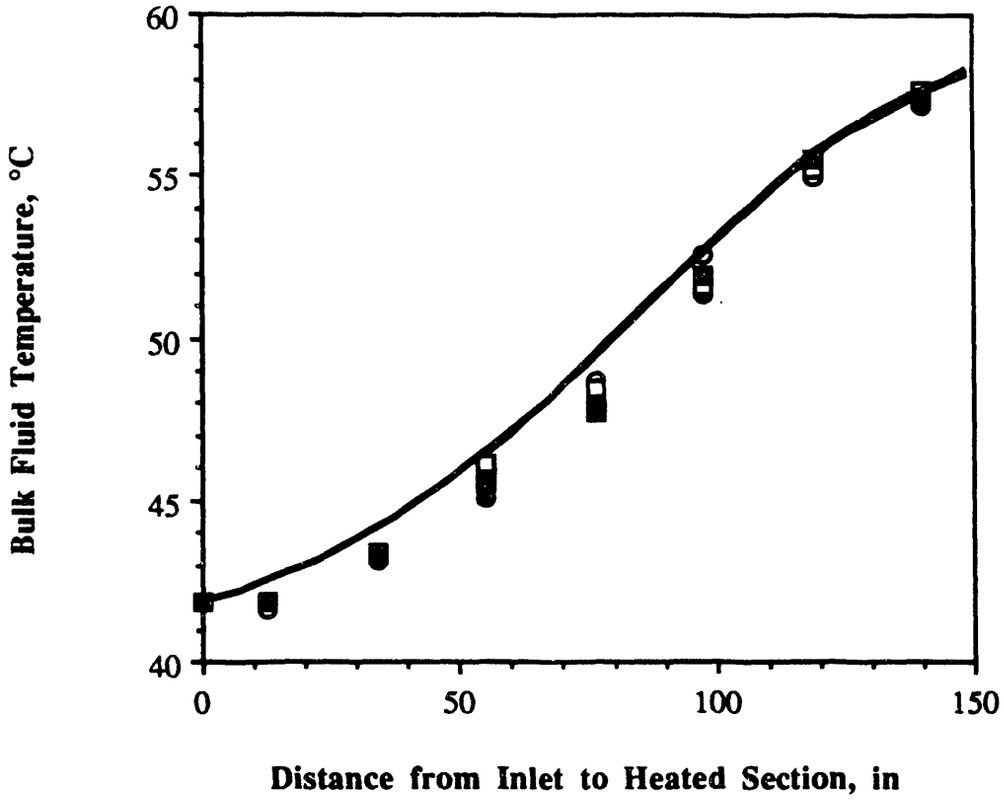

Figure B-4. Comparison of Measured and Calculated Subchannel Fluid Temperatures for the Inner Channel for the SPRIHTE Test at 10 gpm, 40°C Inlet, and 51 kW.

Symbols represent inner channel fluid temperature measurements for the four subchannels. Lines represent calculated inner channel fluid temperatures for the four subchannels. (Calculated temperature profiles for two or more subchannels may coincide because of assumed symmetries in the model.) No correspondence between calculated temperature profiles and specific subchannel measurements is implied.

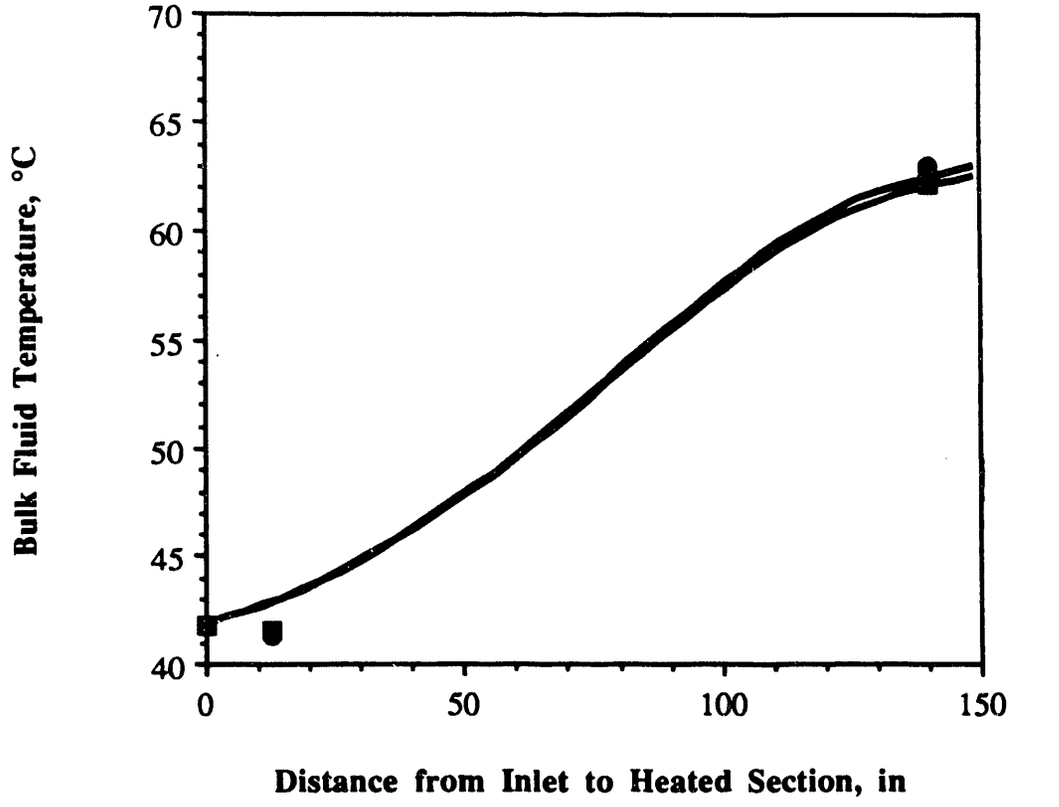

Figure B-5. Comparison of Measured and Calculated Subchannel Fluid Temperatures for the Middle Channel for the SPRIHTE Test at 10 gpm, 40°C Inlet, and 51 kW.

Symbols represent middle channel fluid temperature measurements for the four subchannels. Lines represent calculated middle channel fluid temperatures for the four subchannels. (Calculated temperature profiles for two or more subchannels may coincide because of assumed symmetries in the model.) No correspondence between calculated temperature profiles and specific subchannel measurements is implied.

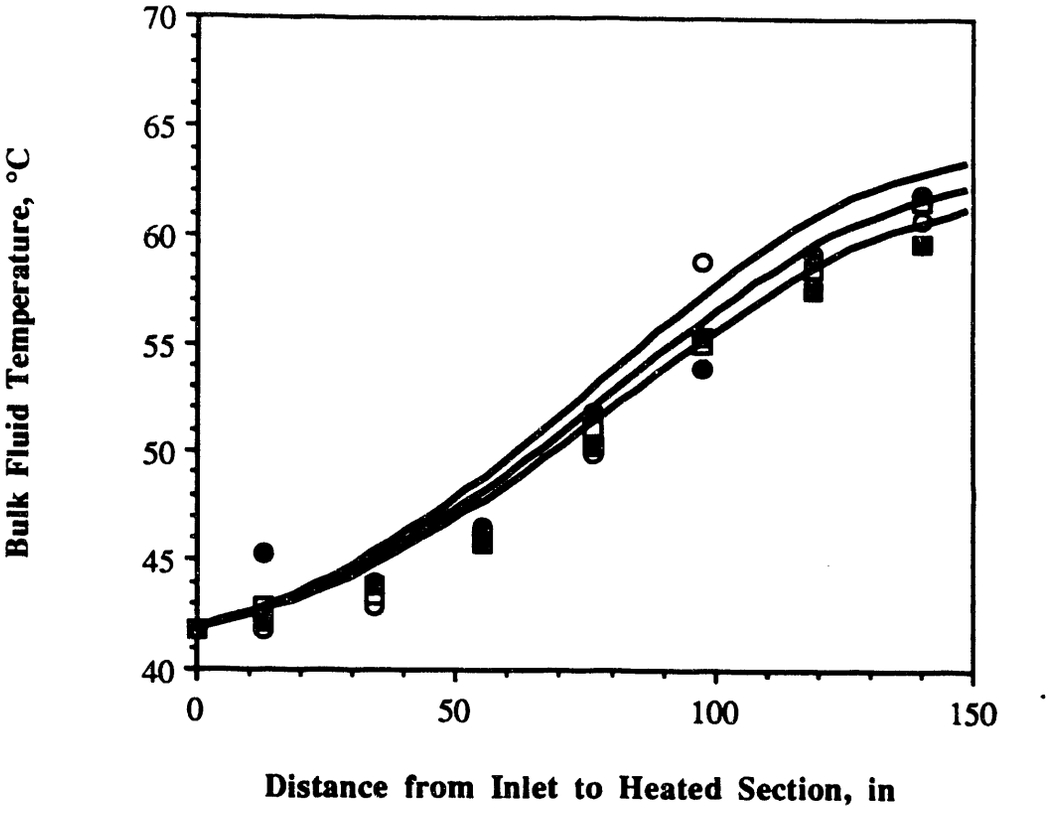

Figure B-6. Comparison of Measured and Calculated Subchannel Fluid Temperatures for the Outer Channel for the SPRIHTE Test at 10 gpm, 40°C Inlet, and 51 kW.

Symbols represent outer channel fluid temperature measurements for the four subchannels. Lines represent calculated outer channel fluid temperatures for the four subchannels. (Calculated temperature profiles for two or more subchannels may coincide because of assumed symmetries in the model.) No correspondence between calculated temperature profiles and specific subchannel measurements is implied.

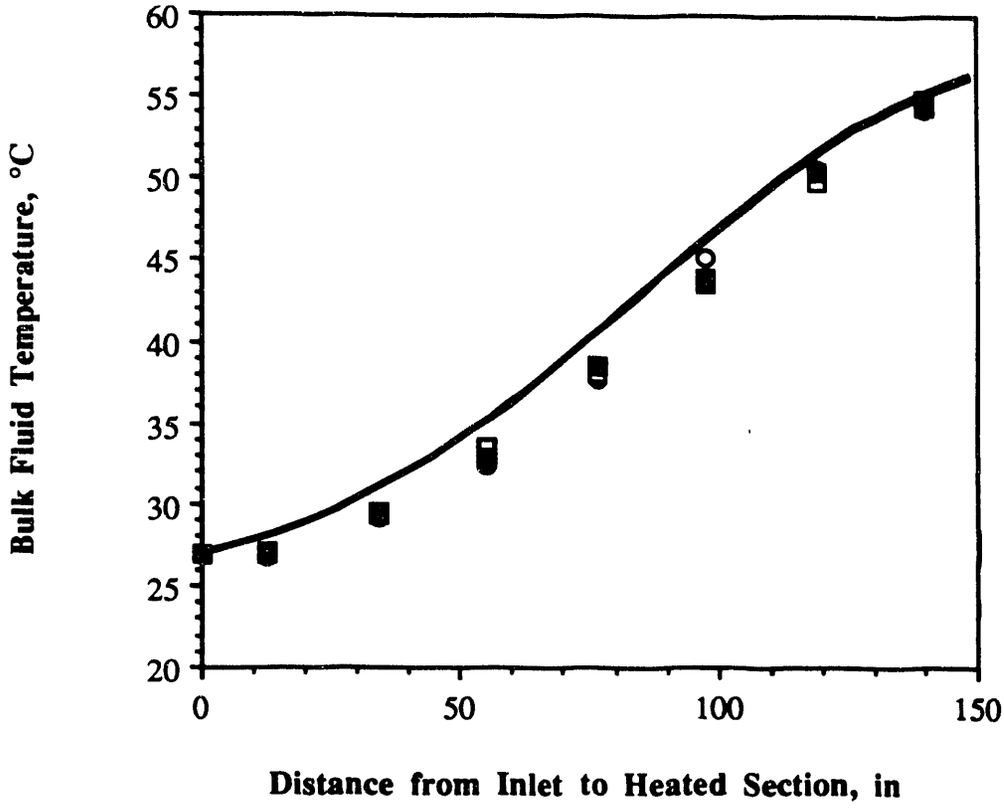

Figure B-7. Comparison of Measured and Calculated Subchannel Fluid Temperatures for the Inner Channel for the SPRIHTE Test at 15 gpm, 25°C Inlet, and 141 kW.

Symbols represent inner channel fluid temperature measurements for the four subchannels. Lines represent calculated inner channel fluid temperatures for the four subchannels. (Calculated temperature profiles for two or more subchannels may coincide because of assumed symmetries in the model.) No correspondence between calculated temperature profiles and specific subchannel measurements is implied.

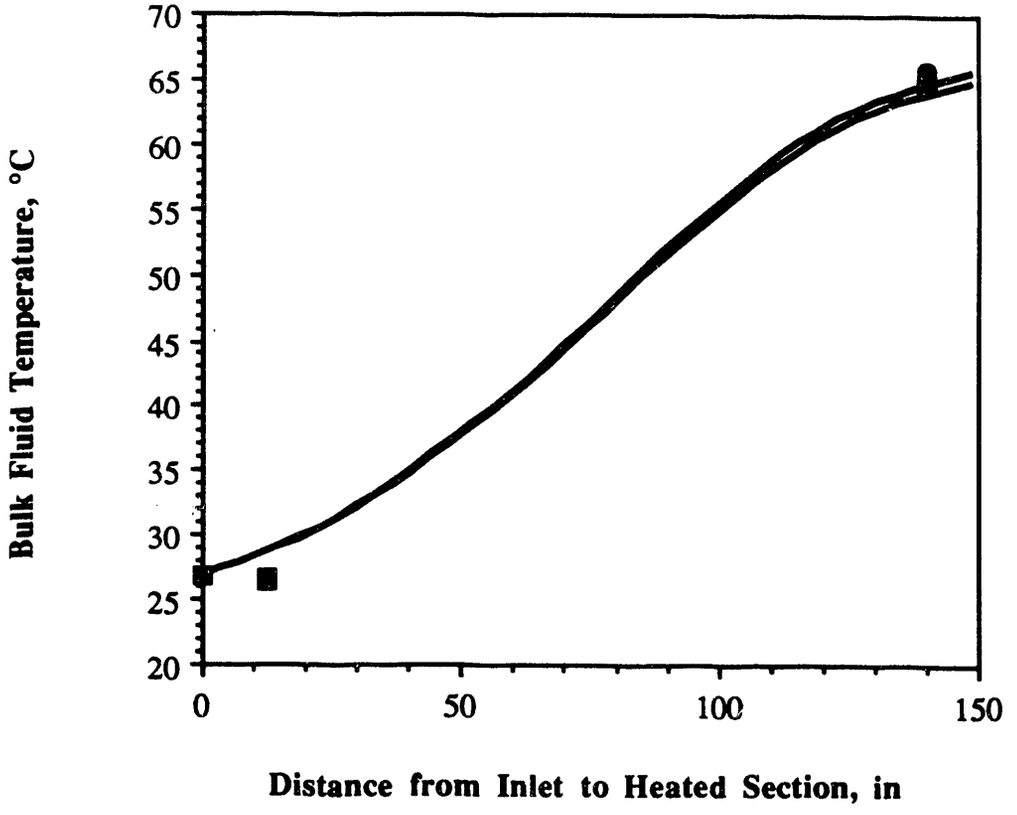

Figure B-8. Comparison of Measured and Calculated Subchannel Fluid Temperatures for the Middle Channel for the SPRIHTE Test at 15 gpm, 25°C Inlet, and 141 kW.

Symbols represent middle channel fluid temperature measurements for the four subchannels. Lines represent calculated middle channel fluid temperatures for the four subchannels. (Calculated temperature profiles for two or more subchannels may coincide because of assumed symmetries in the model.) No correspondence between calculated temperature profiles and specific subchannel measurements is implied.

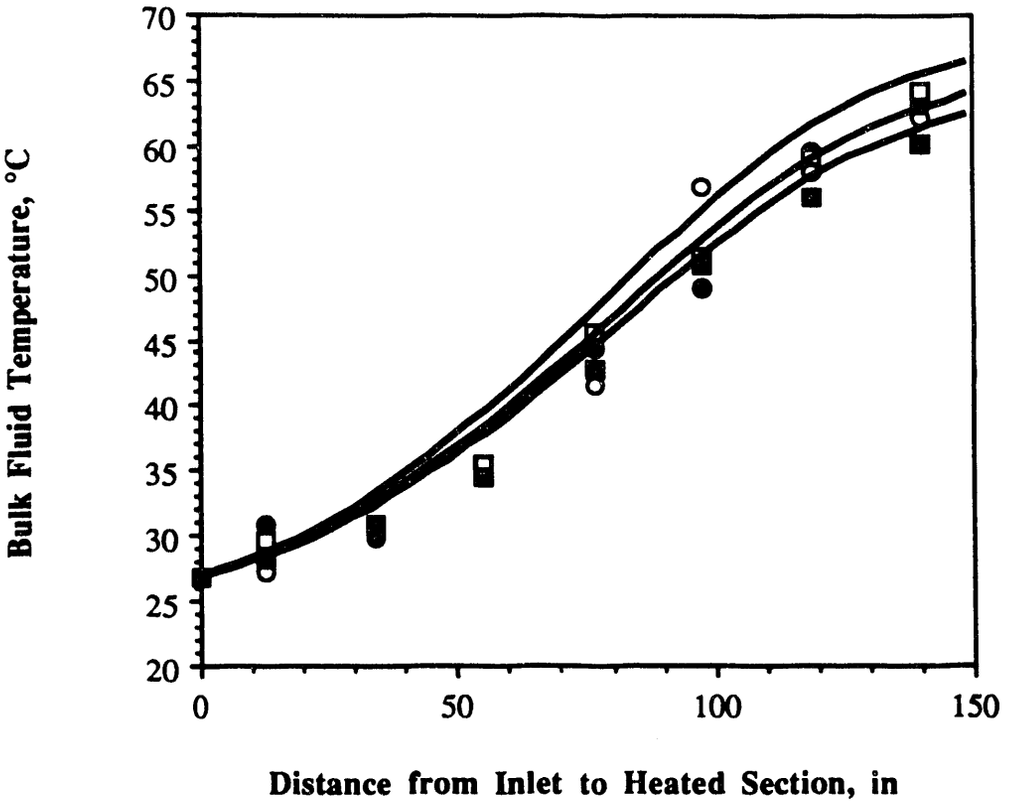

Figure B-9. Comparison of Measured and Calculated Subchannel Fluid Temperatures for the Outer Channel for the SPRIHTE Test at 15 gpm, 25°C Inlet, and 141 kW.

Symbols represent outer channel fluid temperature measurements for the four subchannels. Lines represent calculated outer channel fluid temperatures for the four subchannels. (Calculated temperature profiles for two or more subchannels may coincide because of assumed symmetries in the model.) No correspondence between calculated temperature profiles and specific subchannel measurements is implied.

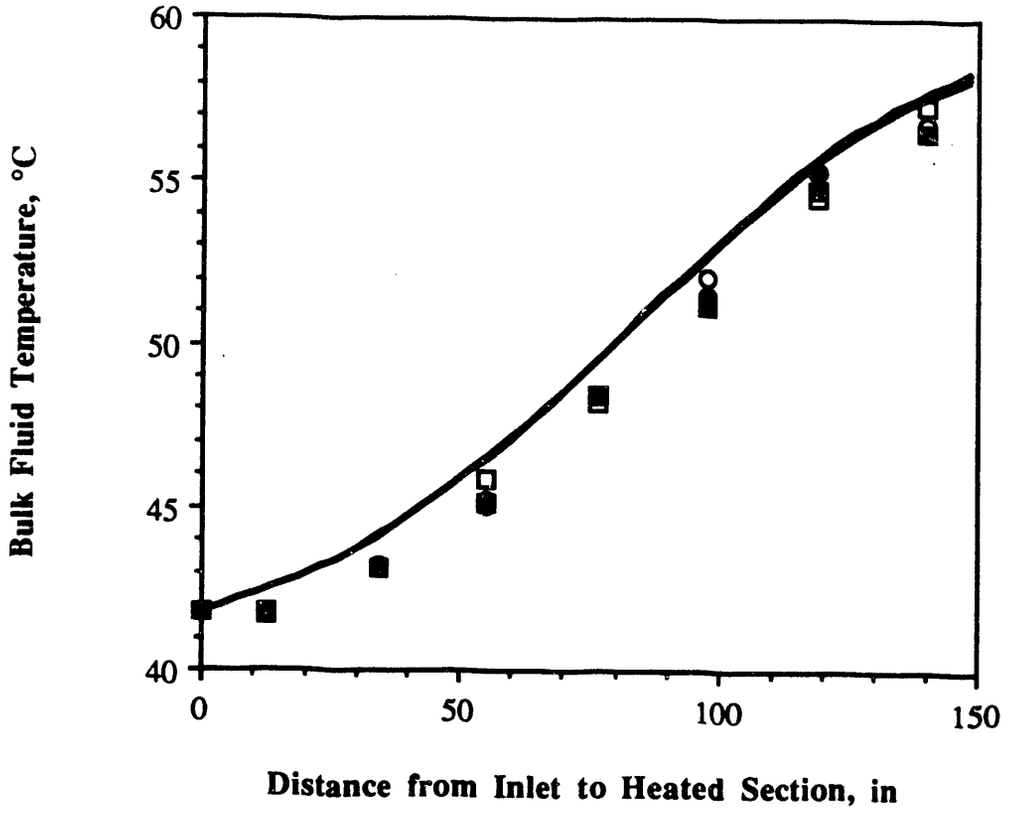

Figure B-10. Comparison of Measured and Calculated Subchannel Fluid Temperatures for the Inner Channel for the SPRIHTE Test at 15 gpm, 40°C Inlet, and 78 kW.

Symbols represent inner channel fluid temperature measurements for the four subchannels. Lines represent calculated inner channel fluid temperatures for the four subchannels. (Calculated temperature profiles for two or more subchannels may coincide because of assumed symmetries in the model.) No correspondence between calculated temperature profiles and specific subchannel measurements is implied.

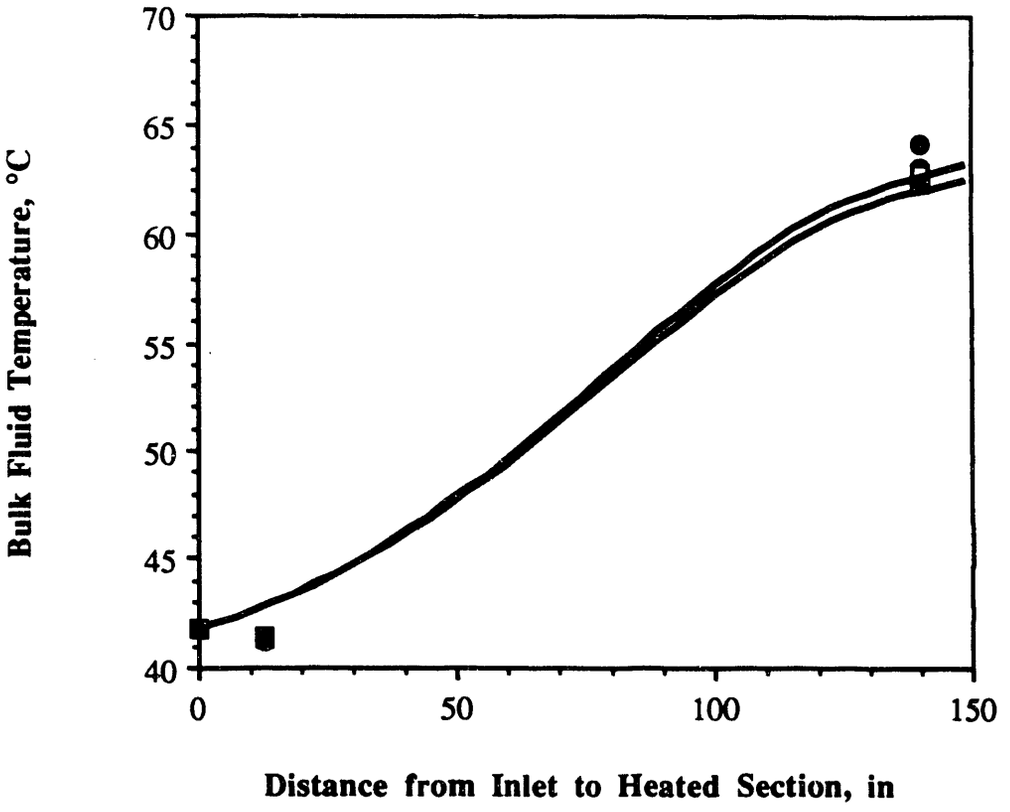

Figure B-11. Comparison of Measured and Calculated Subchannel Fluid Temperatures for the Middle Channel for the SPRIHTE Test at 15 gpm, 40°C Inlet, and 78 kW.

Symbols represent middle channel fluid temperature measurements for the four subchannels. Lines represent calculated middle channel fluid temperatures for the four subchannels. (Calculated temperature profiles for two or more subchannels may coincide because of assumed symmetries in the model.) No correspondence between calculated temperature profiles and specific subchannel measurements is implied.

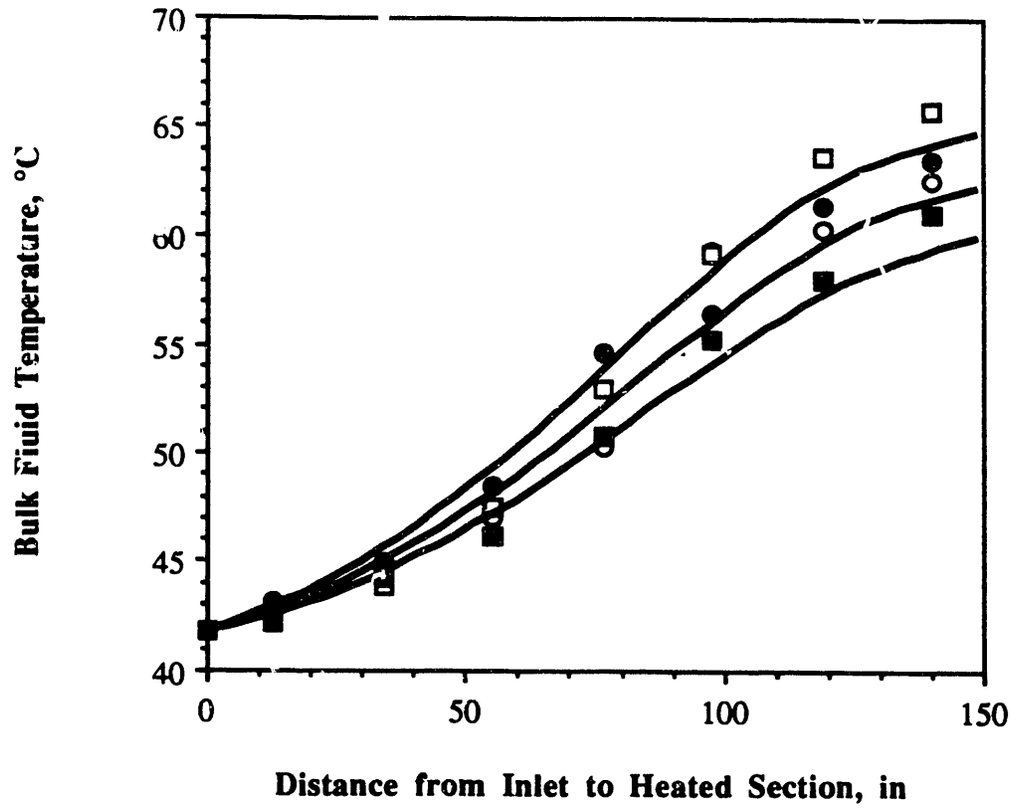

Figure B-12. Comparison of Measured and Calculated Subchannel Fluid Temperatures for the Outer Channel for the SPRIHTE Test at 15 gpm, 40°C Inlet, and 78 kW.

Symbols represent outer channel fluid temperature measurements for the four subchannels. Lines represent calculated outer channel fluid temperatures for the four subchannels. (Calculated temperature profiles for two or more subchannels may coincide because of assumed symmetries in the model.) No correspondence between calculated temperature profiles and specific subchannel measurements is implied.

Appendix C: Comparisons of Measured and Calculated Heater Wall Temperatures

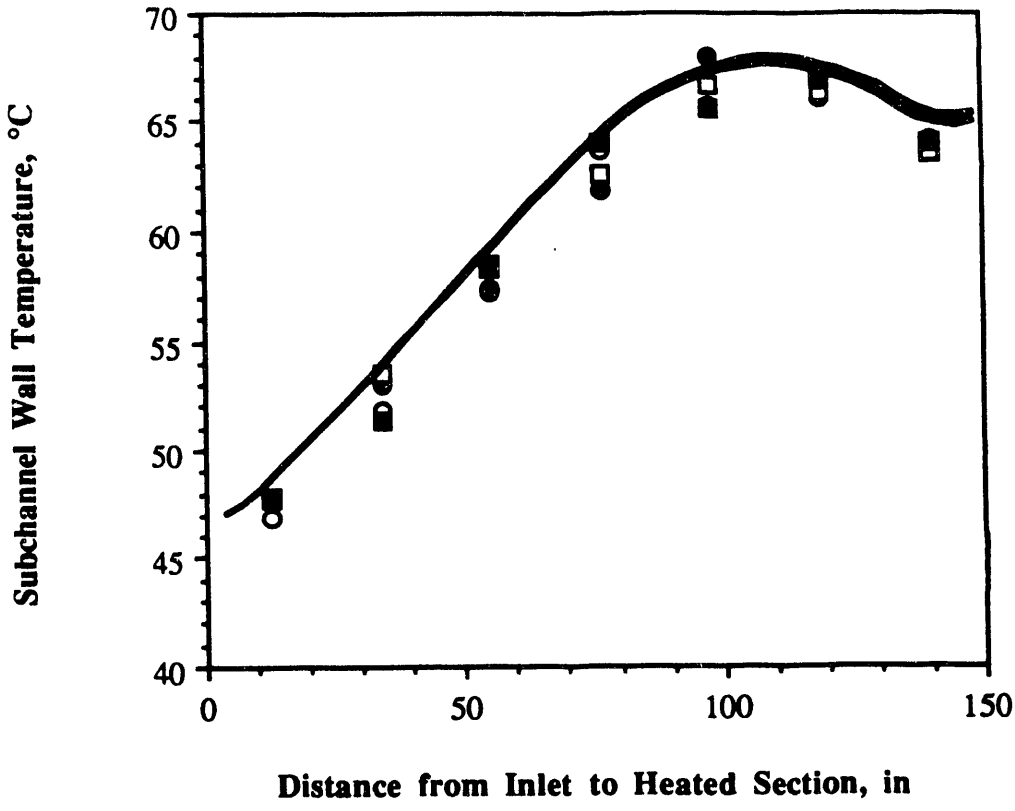

Figure C-1. Comparison of Measured and Calculated Inner Heater Wall Temperatures for the SPRIHTE Test at 15 gpm, 40°C Inlet, and 78 kW.

Symbols represent inner heater wall temperature measurements for the four subchannels. Lines represent calculated inner heater wall temperatures for the four subchannels. (Calculated temperature profiles for two or more subchannels may coincide because of assumed symmetries in the model.) No correspondence between calculated temperature profiles and specific subchannel measurements is implied.

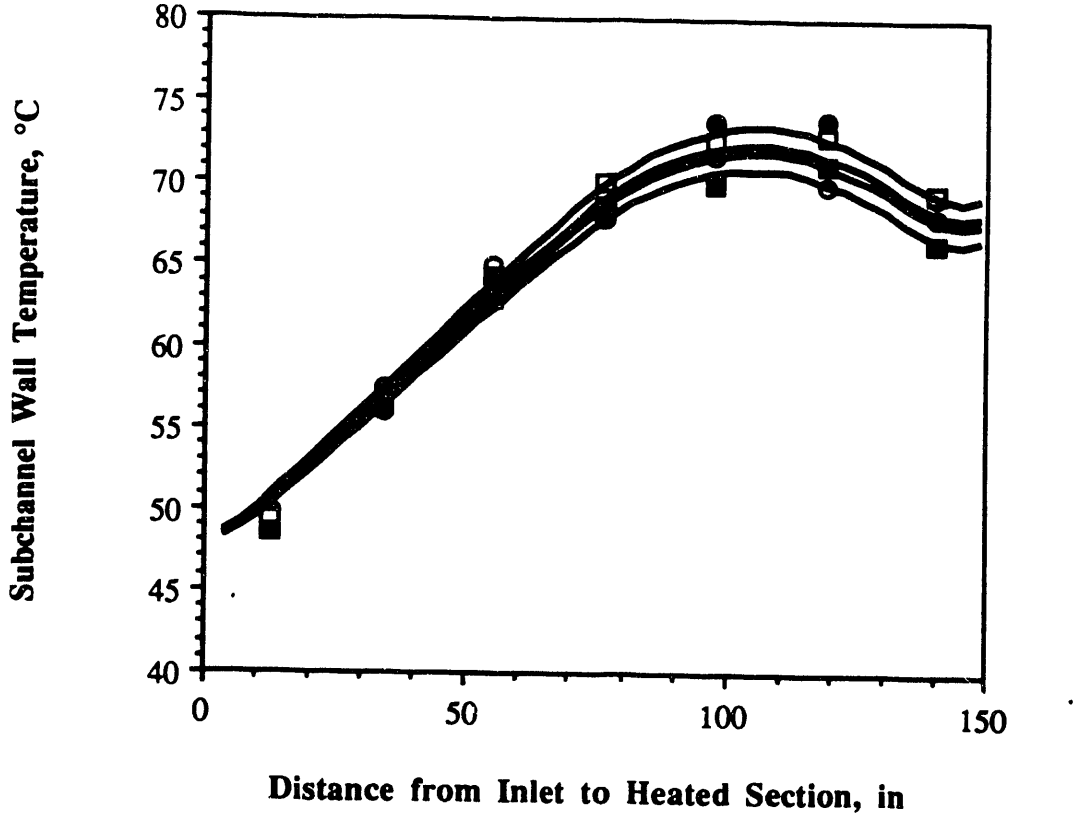

Figure C-2. Comparison of Measured and Calculated Outer Heater Wall Temperatures for the SPRIHTE Test at 15 gpm, 40°C Inlet, and 78 kW.

Symbols represent outer heater wall temperature measurements for the four subchannels. Lines represent calculated outer heater wall temperatures for the four subchannels. (Calculated temperature profiles for two or more subchannels may coincide because of assumed symmetries in the model.) No correspondence between calculated temperature profiles and specific subchannel measurements is implied.

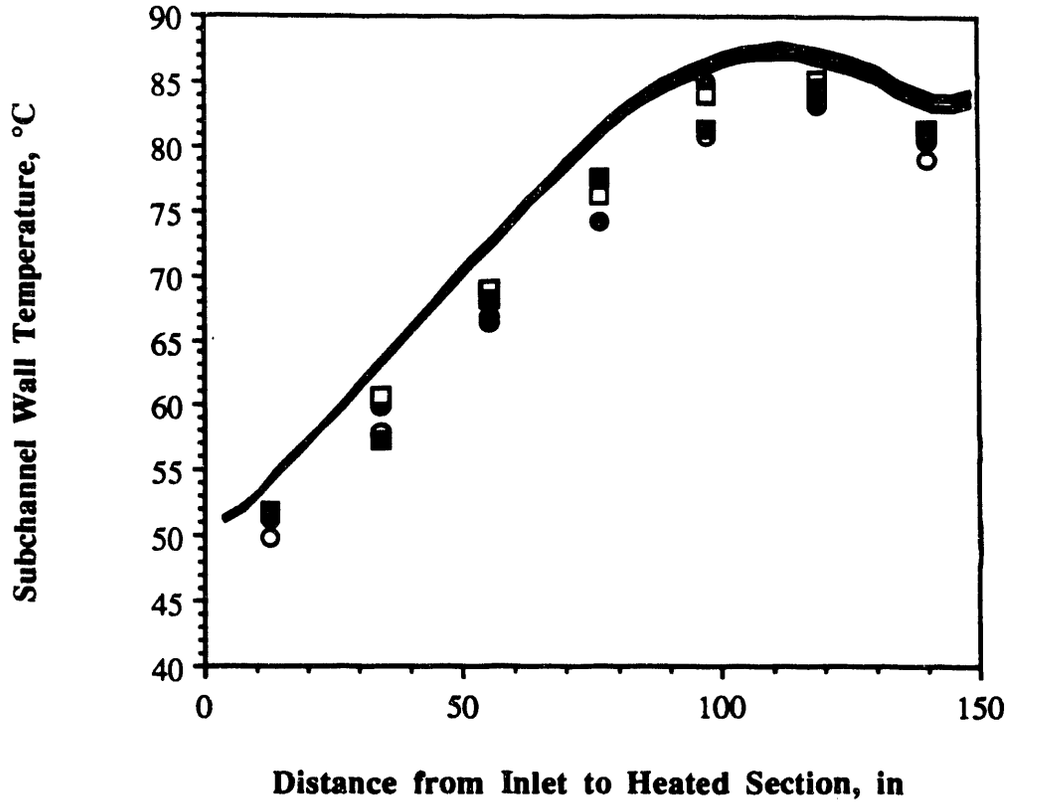

Figure C-3. Comparison of Measured and Calculated Inner Heater Wall Temperatures for the SPRIHTE Test at 15 gpm, 40°C Inlet, and 142 kW.

Symbols represent inner heater wall temperature measurements for the four subchannels. Lines represent calculated inner heater wall temperatures for the four subchannels. (Calculated temperature profiles for two or more subchannels may coincide because of assumed symmetries in the model.) No correspondence between calculated temperature profiles and specific subchannel measurements is implied.

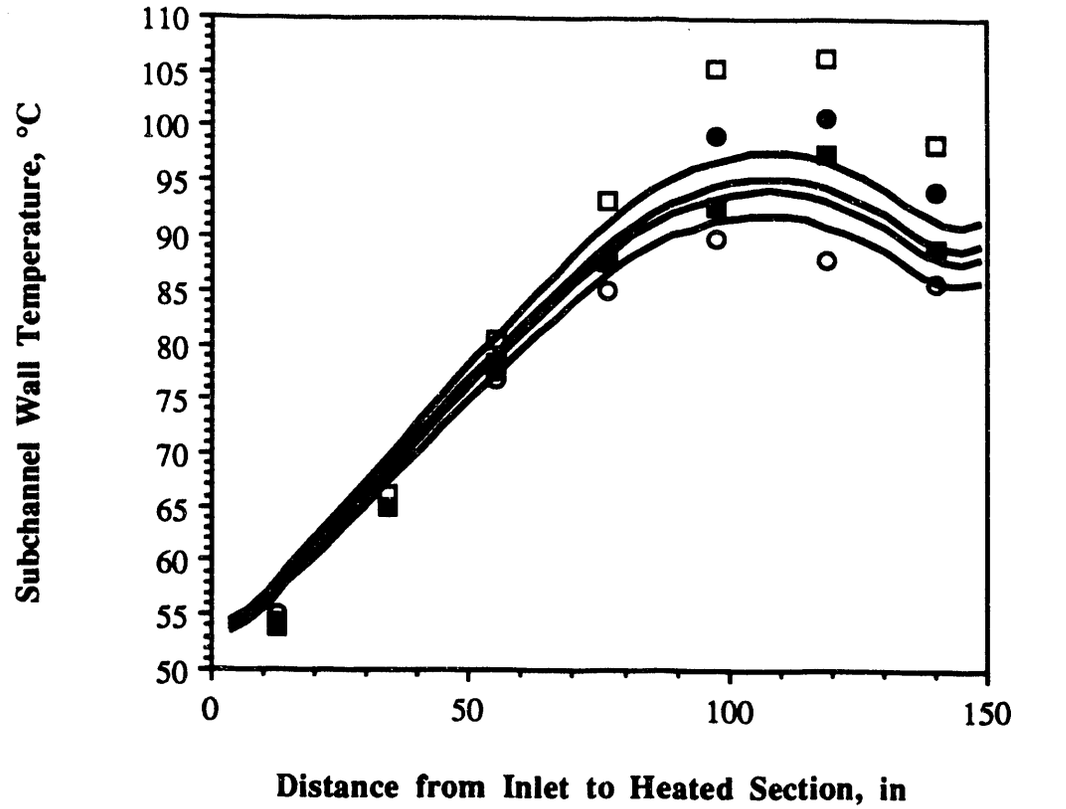

Figure C-4. Comparison of Measured and Calculated Outer Heater Wall Temperatures for the SPRIHTE Test at 15 gpm, 40°C Inlet, and 142 kW.

Symbols represent outer heater wall temperature measurements for the four subchannels. Lines represent calculated outer heater wall temperatures for the four subchannels. (Calculated temperature profiles for two or more subchannels may coincide because of assumed symmetries in the model.) No correspondence between calculated temperature profiles and specific subchannel measurements is implied.

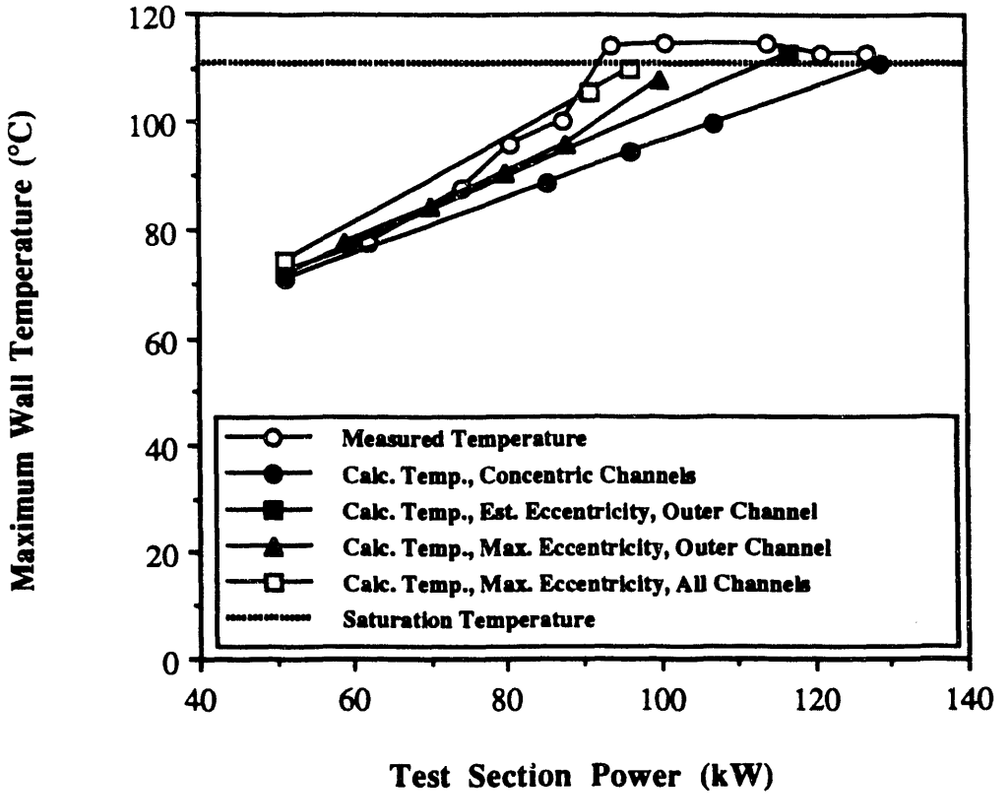

Figure D-2. Comparison of Measured and Calculated Maximum Wall Temperatures for the SPRIHTE Tests at 10 gpm and 40°C Inlet.

Wall temperature calculations were performed for the following subchannel dimensions: 1) concentric flow channels, 2) an outer channel eccentricity set to match computed and measured values for the difference between the hottest and coldest subchannel effluent temperatures, 3) the maximum allowable outer channel eccentricity based on the nominal rib tip clearance, and 4) the maximum allowable eccentricity based on the nominal rib tip clearance for all channels.

Appendix D: Comparisons of Measured and Calculated Maximum Wall Temperatures

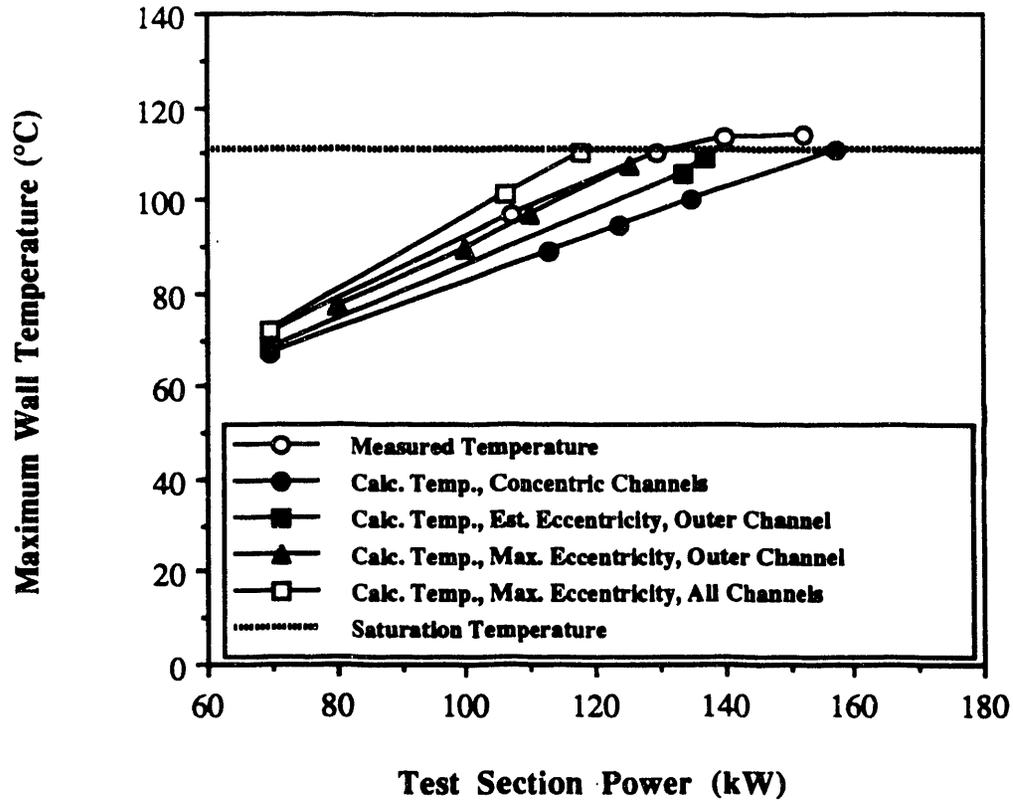

Figure D-1. Comparison of Measured and Calculated Maximum Wall Temperatures for the SPRIHTE Tests at 10 gpm and 25°C Inlet.

Wall temperature calculations were performed for the following subchannel dimensions: 1) concentric flow channels, 2) an outer channel eccentricity set to match computed and measured values for the difference between the hottest and coldest subchannel effluent temperatures, 3) the maximum allowable outer channel eccentricity based on the nominal rib tip clearance, and 4) the maximum allowable eccentricity based on the nominal rib tip clearance for all channels.

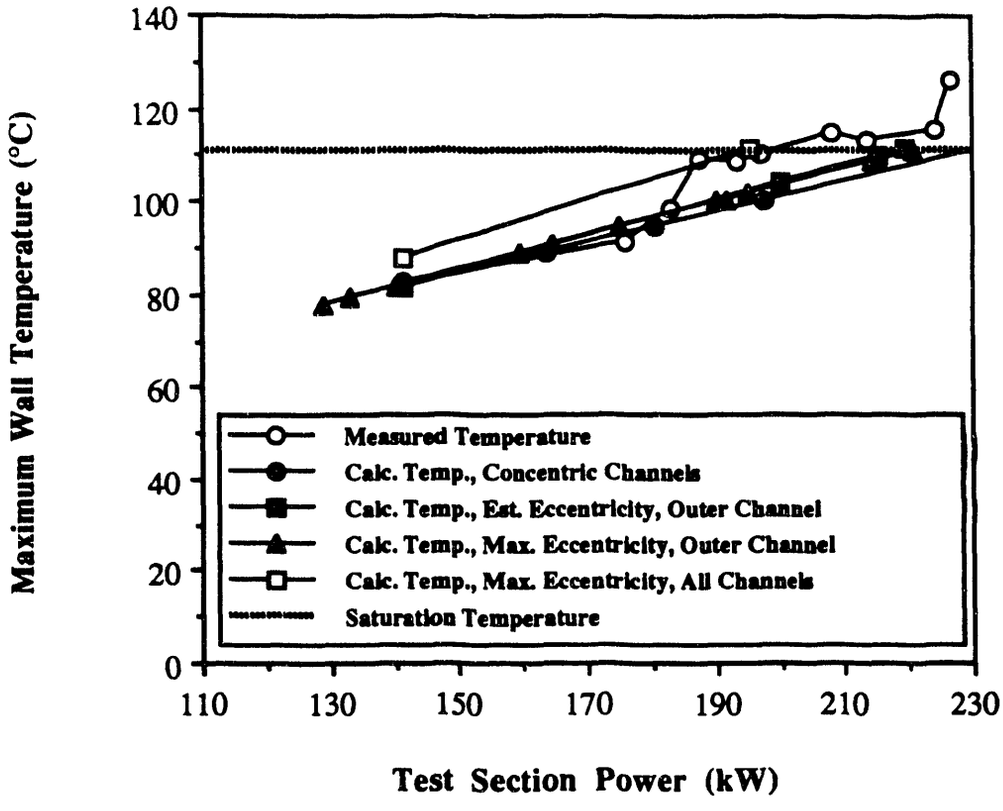

Figure D-3. Comparison of Measured and Calculated Maximum Wall Temperatures for the SPRIHTE Tests at 15 gpm and 25°C Inlet.

Wall temperature calculations were performed for the following subchannel dimensions: 1) concentric flow channels, 2) an outer channel eccentricity set to match computed and measured values for the difference between the hottest and coldest subchannel effluent temperatures, 3) the maximum allowable outer channel eccentricity based on the nominal rib tip clearance, and 4) the maximum allowable eccentricity based on the nominal rib tip clearance for all channels.

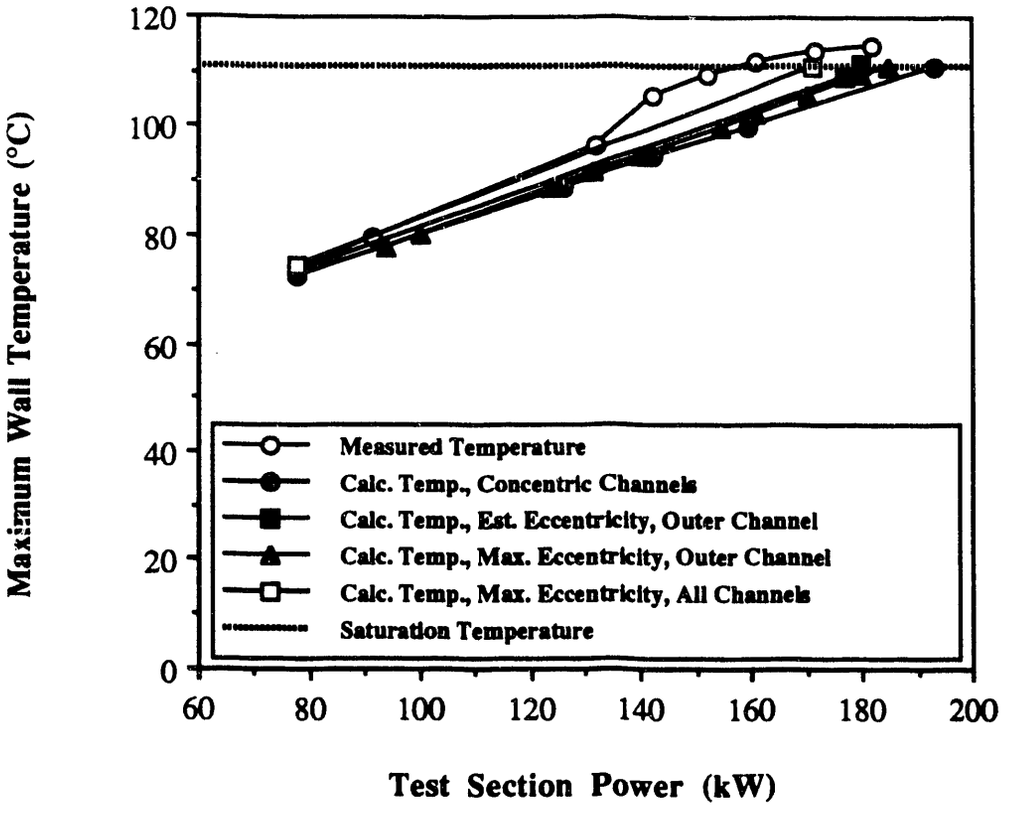

Figure D-4. Comparison of Measured and Calculated Maximum Wall Temperatures for the SPRIHTE Tests at 15 gpm and 40°C Inlet.

Wall temperature calculations were performed for the following subchannel dimensions: 1) concentric flow channels, 2) an outer channel eccentricity set to match computed and measured values for the difference between the hottest and coldest subchannel effluent temperatures, 3) the maximum allowable outer channel eccentricity based on the nominal rib tip clearance, and 4) the maximum allowable eccentricity based on the nominal rib tip clearance for all channels.

END

DATE FILMED

9/29/93